UNIVERSITY OF AMSTERDAM

UvA-DARE (Digital Academic Repository)

Measurements of the production cross section of a Z boson in association with jets in pp collisions at √s =13 TeV with the ATLAS detector

ATLAS Collaboration

DOI
10.1140/epjc/s10052-017-4900-z

Publication date
2017

Document Version
Final published version

Published in
European Physical Journal C

License
CC BY

Link to publication

Citation for published version (APA):
ATLAS Collaboration (2017). Measurements of the production cross section of a *Z* boson in association with jets in *pp* collisions at √*s* =13 TeV with the ATLAS detector. *European Physical Journal C*, *77*(6), Article 361. https://doi.org/10.1140/epjc/s10052-017-4900-z

General rights
It is not permitted to download or to forward/distribute the text or part of it without the consent of the author(s) and/or copyright holder(s), other than for strictly personal, individual use, unless the work is under an open content license (like Creative Commons).

Disclaimer/Complaints regulations
If you believe that digital publication of certain material infringes any of your rights or (privacy) interests, please let the Library know, stating your reasons. In case of a legitimate complaint, the Library will make the material inaccessible and/or remove it from the website. Please Ask the Library: https://uba.uva.nl/en/contact, or a letter to: Library of the University of Amsterdam, Secretariat, P.O. Box 19185, 1000 GD Amsterdam, The Netherlands. You will be contacted as soon as possible.

UvA-DARE is a service provided by the library of the University of Amsterdam (https://dare.uva.nl)

Download date:12 Nov 2026

Eur. Phys. J. C (2017) 77:361
DOI 10.1140/epjc/s10052-017-4900-z

THE EUROPEAN PHYSICAL JOURNAL C

CrossMark

Regular Article - Experimental Physics

Measurements of the production cross section of a Z boson in association with jets in pp collisions at $\sqrt{s} = 13$ TeV with the ATLAS detector

ATLAS Collaboration[⋆]

CERN, 1211 Geneva 23, Switzerland

Received: 21 February 2017 / Accepted: 8 May 2017 / Published online: 31 May 2017
© CERN for the benefit of the ATLAS collaboration 2017. This article is an open access publication

Abstract Measurements of the production cross section of a Z boson in association with jets in proton–proton collisions at $\sqrt{s} = 13$ TeV are presented, using data corresponding to an integrated luminosity of 3.16 fb^{-1} collected by the ATLAS experiment at the CERN Large Hadron Collider in 2015. Inclusive and differential cross sections are measured for events containing a Z boson decaying to electrons or muons and produced in association with up to seven jets with $p_{\mathrm{T}} > 30$ GeV and $|y| < 2.5$. Predictions from different Monte Carlo generators based on leading-order and next-to-leading-order matrix elements for up to two additional partons interfaced with parton shower and fixed-order predictions at next-to-leading order and next-to-next-to-leading order are compared with the measured cross sections. Good agreement within the uncertainties is observed for most of the modelled quantities, in particular with the generators which use next-to-leading-order matrix elements and the more recent next-to-next-to-leading-order fixed-order predictions.

Contents

1 Introduction . . . 1
2 The ATLAS detector . . . 2
3 Data set, simulated event samples, and predictions . . . 2
3.1 Data set . . . 2
3.2 Simulated event samples . . . 2
3.3 Fixed-order predictions . . . 4
4 Event selection . . . 4
4.1 Correction factors and related systematic uncertainties . . . 5
5 Background estimation . . . 6
5.1 Top-quark and electroweak backgrounds . . . 6
5.2 Multijet background . . . 7
6 Kinematic distributions . . . 7
7 Unfolding of detector effects . . . 7
7.1 Systematic uncertainties associated with the unfolding procedure . . . 10
8 Results . . . 10
8.1 Results in the individual channels and the combination . . . 11
8.2 Comparisons of results to predictions . . . 12
9 Conclusion . . . 15
References . . . 16

1 Introduction

The measurement of the production of a Z boson[1] in association with jets, Z + jets, constitutes a powerful test of perturbative quantum chromodynamics (QCD) [1,2]. The large production cross section and easily identifiable decays of the Z boson to charged leptonic final states offer clean experimental signatures which can be precisely measured. Such processes also constitute a non-negligible background for studies of the Higgs boson and in searches for new phenomena; typically in these studies, the multiplicity and kinematics of the jets are exploited to achieve a separation of the signal of interest from the Standard Model (SM) Z + jets process. These quantities are often measured in control regions and subsequently extrapolated to the signal region with the use of Monte Carlo (MC) generators, which are themselves subject to systematic uncertainty and must be tuned and validated using data. Predictions from the most recent generators combine next-to-leading-order (NLO) multi-leg matrix elements with a parton shower (PS) and a hadronisation model. Fixed-order parton-level predictions for Z + jets production at next-to-next-to-leading order (NNLO) are also available [3–6].

The Z + jets production differential cross section was previously measured by the ATLAS [7], CMS [8], and

⋆ e-mail: atlas.publications@cern.ch

[1] Throughout this paper, Z/γ^*-boson production is denoted simply by Z-boson production.

LHCb [9] collaborations at the CERN Large Hadron Collider (LHC) [10] at centre-of-mass energies of $\sqrt{s} = 7$ TeV [11–15] and 8 TeV [16–18], and by the CDF and D0 collaborations at the Tevatron collider at $\sqrt{s} = 1.96$ TeV [19,20]. In this paper, proton–proton (pp) collision data corresponding to an integrated luminosity of 3.16 fb^{-1}, collected at $\sqrt{s} = 13$ TeV with the ATLAS detector during 2015, are used for measurements of the Z-boson production cross section in association with up to seven jets within a fiducial region defined by the detector acceptance. The Z boson is identified using its decays to electron or muon pairs ($Z \to e^+e^-$, $Z \to \mu^+\mu^-$). Cross sections are measured separately for these two channels, and for their combination, as a function of the inclusive and exclusive jet multiplicity N_{jets} and the ratio of successive inclusive jet multiplicities $(N_{\text{jets}} + 1)/N_{\text{jets}}$, the transverse momentum of the leading jet $p_{\text{T}}^{\text{jet}}$ for several jet multiplicities, the jet rapidity y^{jet}, the azimuthal separation between the two leading jets $\Delta\phi_{\text{jj}}$, the two leading jet invariant mass m_{jj}, and the scalar sum H_{T} of the transverse momenta of all selected leptons and jets.

The paper is organised as follows. Section 2 contains a brief description of the ATLAS detector. The data and simulated samples as well as the Z + jets predictions used in the analysis are described in Sect. 3. The event selection and its associated uncertainties are presented in Sect. 4, while the methods employed to estimate the backgrounds are shown in Sect. 5. Comparisons between data and Monte Carlo predictions for reconstructed distributions are found in Sect. 6, while the unfolding procedure is described in Sect. 7. Section 8 presents the analysis results, the comparisons to predictions, and a discussion of their interpretation. Conclusions are provided in Sect. 9.

2 The ATLAS detector

The ATLAS experiment at the LHC is a multi-purpose particle detector with a forward-backward symmetric cylindrical geometry and nearly 4π coverage in solid angle.[2] It consists of an inner tracking detector, electromagnetic and hadronic calorimeters, and a muon spectrometer. The inner tracker is surrounded by a thin superconducting solenoid magnet and provides precision tracking of charged particles and momentum measurements in the pseudorapidity range $|\eta| < 2.5$. This region is matched to a high-granularity electromagnetic (EM) sampling calorimeter covering the pseudorapidity range $|\eta| < 3.2$, and a coarser granularity calorimeter up to $|\eta| = 4.9$. The hadronic calorimeter system covers the entire pseudorapidity range up to $|\eta| = 4.9$. The muon spectrometer consists of three large superconducting toroids each containing eight coils, a system of trigger chambers, and precision tracking chambers, which provide trigger and tracking capabilities in the range $|\eta| < 2.4$ and $|\eta| < 2.7$, respectively. A two-level trigger system [21] is used to select events. The first-level trigger is implemented in hardware and uses a subset of the detector information. This is followed by the software-based high-level trigger system, which runs offline reconstruction, reducing the event rate to approximately 1 kHz.

3 Data set, simulated event samples, and predictions

3.1 Data set

The data used in this analysis were collected by the ATLAS detector during August to November 2015. During this period, the LHC circulated 6.5 TeV proton beams with a 25 ns bunch spacing. The peak delivered instantaneous luminosity was $L = 5 \times 10^{33}\,\text{cm}^{-2}\,\text{s}^{1}$ and the mean number of pp interactions per bunch crossing (hard scattering and pile-up events) was $\langle\mu\rangle = 13$. The data set used in this measurement corresponds to a total integrated luminosity of 3.16 fb^{-1}.

3.2 Simulated event samples

Monte Carlo simulations, normalised to higher-order calculations, are used to estimate most of the contributions from background events, to unfold the data to the particle level, and to compare with the unfolded data distributions. All samples are processed with a GEANT4-based simulation [22] of the ATLAS detector [23]. An overview of all signal and background processes considered and of the generators used for the simulation is given in Table 1. Total production cross sections for the samples, their respective uncertainties (mainly coming from parton distribution function (PDF) and factorisation and renormalisation scale variations), and references to higher-order QCD corrections, where available, are also listed in Table 1.

Signal events (i.e. containing a Z boson with associated jets) are simulated using the SHERPA v2.2.1 [31] generator, denoted by SHERPA 2.2. Matrix elements (ME) are calculated for up to two additional partons at NLO and up to four partons at leading order (LO) using the Comix [34]

[2] ATLAS uses a right-handed coordinate system with its origin at the nominal interaction point (IP) in the centre of the detector and the z-axis along the beam pipe. The x-axis points from the IP to the centre of the LHC ring, and the y-axis points upwards. Cylindrical coordinates (r, ϕ) are used in the transverse plane, ϕ being the azimuthal angle around the z-axis. The pseudorapidity is defined in terms of the polar angle θ as $\eta = -\ln\tan(\theta/2)$. Angular distance is measured in units of $\Delta R \equiv \sqrt{(\Delta\eta)^2 + (\Delta\phi)^2}$. When dealing with massive jets and particles, the rapidity $y = \frac{1}{2}\ln\left(\frac{E+p_z}{E-p_z}\right)$ is used, where E is the jet/particle energy and p_z is the z-component of the jet/particle momentum.

Table 1 Signal and background Monte Carlo samples and the generators used in the simulation. Each sample is normalised to the appropriate production cross section σ and multiplied by the relevant branching ratios (BR) per lepton flavour for this sample, as shown in the third column. For W-boson and top-quark production, contributions from higher-order QCD corrections were calculated following the references given in the fifth column for the stated order. Similarly, for Z-boson production, higher-order QCD corrections were evaluated in the dilepton invariant mass range $66 < m_{\ell\ell} < 116$ GeV following the references given in the fifth column for the stated order, and extrapolation scaling factors were applied to match mass ranges used by each simulation as given in the first column. The theory uncertainties as given in the final column correspond to PDF and scale variations. The diboson samples include on-shell and off-shell WW, WZ and ZZ production. Recently, NNLO QCD predictions have been made available for the diboson processes [32,33]. However, these higher-order corrections have a negligible impact on this analysis

Process	Generator	$(\sigma \cdot \text{BR})$ [pb]	Normalisation order	References	Theory uncert. (%)
$Z(\to \ell^+\ell^-)$ + jets ($\ell = e, \mu$; $m_{\ell\ell} > 40$ GeV)	SHERPA 2.2	2106	NNLO	[24–27]	5
$Z(\to \ell^+\ell^-)$ + jets ($\ell = e, \mu, \tau$; $m_{\ell\ell} > 40$ GeV)	MG5_aMC@NLO+PY8	2103	NNLO	[24–27]	5
$W \to \ell\nu$ ($\ell = e, \mu$)	MG5_aMC@NLO+PY8	20, 080	NNLO	[24–27]	5
$t\bar{t}$ ($m_t = 172.5$ GeV)					
PERUGIA2012(RADHI/RADLO)	POWHEG+PY6	831	NNLO+NNLL	[28]	6
UE- EE- 5	MG5_aMC@NLO+Herwig++	831	NNLO+NNLL	[28]	6
Single top quark (Wt)	POWHEG+PY6	72	NLO+NNLL	[29]	6
Single top quark (t-channel)	POWHEG+PY6	136	NLO+NNLL	[30]	6
Single top anti-quark (t-channel)	POWHEG+PY6	81	NLO+NNLL	[30]	6
Dibosons	SHERPA 2.1	97	NLO	[31]	6

and OpenLoops [35] matrix element generators. They are merged with the SHERPA parton shower [36] (with a matching scale of 20 GeV) using the ME+PS@NLO prescription [37]. A five-flavour scheme is used for these predictions. The NNPDF30NLO PDF set [38] is used in conjunction with a dedicated set of parton-shower-generator parameters (tune) developed by the SHERPA authors. This sample is used for the nominal unfolding of the data distributions, to compare to the cross-section measurements, and to estimate the systematic uncertainties.

A simulated sample of Z + jets production is also produced with the MADGRAPH_aMC@NLO (denoted by MG5_aMC@NLO) v2.2.2 generator [39], using matrix elements including up to four partons at leading order and employing the NNPDF30NLO PDF set, interfaced to PYTHIA v8.186 [40] to model the parton shower, using the CKKWL merging scheme [41] (with a matching scale of 30 GeV). A five-flavour scheme is used. The A14 [42] parton-shower tune is used together with the NNPDF23LO PDF set [43]. The sample is denoted by MG5_aMC+PY8 CKKWL and is used to provide cross-checks of the systematic uncertainty in the unfolding and to model the small $Z \to \tau\tau$ background. In addition, a MG5_aMC@NLO sample with matrix elements for up to two jets and with parton showers beyond this, employing the NNPDF30NLO PDF set and interfaced to PYTHIA v8.186 to model the parton shower, is generated using the FxFx merging scheme [44] (with a matching scale of 25 GeV [45]) and is denoted by MG5_aMC+PY8 FxFx. This sample also uses a five-flavour scheme and the A14 parton-shower tune with the NNPDF23LO PDF set. Both MG5_aMC@NLO samples are used for comparison with the unfolded cross-section measurements.

The measured cross sections are also compared to predictions from the leading-order matrix element generator ALPGEN v2.14 [46] interfaced to PYTHIA v6.426 [47] to model the parton shower, denoted by ALPGEN+PY6, using the PERUGIA2011C [48] parton-shower tune and the CTEQ6L1 PDF set [49]. A four-flavour scheme is used. Up to five additional partons are modelled by the matrix elements merged with the MLM prescription [46] (with a matching scale of 20 GeV). The matrix elements for the production of $Z + b\bar{b}$ and $Z + c\bar{c}$ events are explicitly included and a heavy-flavour overlap procedure is used to remove the double counting of heavy quarks from gluon splitting in the parton shower.

The Z-boson samples are normalised to the NNLO prediction calculated with the Fewz 3.1 program [24–27] with CT10NNLO PDFs [50].

Contributions from the top-quark, single-boson, and diboson components of the background (described in Sect. 5) are estimated from the following Monte Carlo samples. Samples of top-quark pair and single top-quark production are generated at NLO with the POWHEG-Box generator [51–53] [versions v2 (r3026) for top-quark pairs and v1 for single top quarks (r2556 and r2819 for t-and Wt-channels, respectively)] and PYTHIA v6.428 (PERUGIA2012 tune [48]). Samples with enhanced or suppressed additional

radiation are generated with the PERUGIA2012RADHI/LO tunes [48]. An alternative top-quark pair sample is produced using the MG5_aMC@NLO generator interfaced with Herwig++ v2.7.1 [39,54], using the UE- EE- 5 tune [55]. The samples are normalised to the cross section calculated at NNLO+NNLL (next-to-next-to-leading log) with the Top++2.0 program [28].

The W-boson backgrounds are modelled using the MG5_aMC+PY8 CKKWL v2.2.2 generator, interfaced to PYTHIA v8.186 and are normalised to the NNLO values given in Table 1. Diboson processes with fully leptonic and semileptonic decays are simulated [56] using the SHERPA v2.1.1 generator with the CT10NLO PDF set. The matrix elements contain the doubly resonant WW, WZ and ZZ processes, and all other diagrams with four electroweak vertices. They are calculated for one or zero additional partons at NLO and up to three additional partons at LO and merged with the SHERPA parton shower using the ME+PS@NLO prescription.

Events involving semileptonic decays of heavy quarks, hadrons misidentified as leptons, and, in the case of the electron channel, electrons from photon conversions are referred to collectively as "multijet events". The multijet background was estimated using data-driven techniques, as described in Sect. 5.

Multiple overlaid pp collisions are simulated with the soft QCD processes of PYTHIA v.8.186 using the A2 tune [57] and the MSTW2008LO PDF set [58]. All Monte Carlo samples are reweighted so that the pile-up distribution matches that observed in the data.

3.3 Fixed-order predictions

In addition to these Monte Carlo samples, parton-level fixed-order predictions at NLO are calculated by the BLACKHAT+SHERPA collaboration for the production of Z bosons with up to four partons [59,60]. The BLACKHAT+SHERPA predictions use the CT14 PDF set [61] including variations of its eigenvectors at the 68% confidence level, rescaled from 90% confidence level using a factor of 1/1.645. The nominal predictions use a factorisation and renormalisation scale of $H_{\mathrm{T}}/2$ with uncertainties derived from the envelope of a common variation of the scales by factors of 0.5, $1/\sqrt{2}$, $\sqrt{2}$, and 2. The effects of PDF and scale uncertainties range from 1 to 4% and from 0.1 to 10%, respectively, for the cross sections of Z-boson production in association with at least one to four partons, and are included in the predictions which are provided by the BLACKHAT+SHERPA authors for the fiducial phase space of this analysis. Since these predictions are defined before the decay leptons emit photons via final-state radiation (Born-level FSR), corrections to the dressed level (where all photons found within a cone of size $\Delta R = 0.1$ of the lepton from the decay of the Z boson are included) are derived from MG5_aMC+PY8 CKKWL, separately for each kinematic observable used to measure cross sections, with associated systematic uncertainties obtained by comparing to the ALPGEN+PY6 generator. This correction is needed in order to match the prediction to the lepton definition used in the measurements. The average size of these corrections is approximately -2%. To bring the prediction from parton to particle level, corrections for the non-perturbative effects of hadronisation and the underlying event are also calculated separately for each observable using the SHERPA v2.2 generator by turning on and off in the simulation both the fragmentation and the interactions between the proton remnants. The net size of the corrections is up to approximately 10% at small values of $p_{\mathrm{T}}^{\mathrm{jet}}$ and vanishes for large values of $p_{\mathrm{T}}^{\mathrm{jet}}$. An uncertainty of approximately 2% for this correction is included in the total systematic uncertainty of the prediction.

Calculations of cross sections at NNLO QCD have recently become available [3–6]. In this paper, the results are compared to the calculation, denoted by $Z+\geq 1$ jet $\mathrm{N_{jetti}}$ NNLO [3,4], which uses a new subtraction technique based on *N-jettiness* [62] and relies on the theoretical formalism provided in soft-collinear effective theory. The predictions, which are provided by the authors of this calculation for the fiducial phase space of this analysis, use a factorisation and renormalisation scale of $\sqrt{m_{\ell\ell}^2 + \sum \left(p_{\mathrm{T}}^{\mathrm{jet}}\right)^2}$ (where $m_{\ell\ell}$ is the invariant mass of the dilepton system) and the CT14 PDF set. The QCD renormalisation and factorisation scales were jointly varied by a common factor of two, and are included in the uncertainties. Non-perturbative and FSR corrections and their associated uncertainties as discussed above are also included in the predictions.

4 Event selection

Electron- and muon-candidate events are selected using triggers which require at least one electron or muon with transverse momentum thresholds of $p_{\mathrm{T}} = 24\,\mathrm{GeV}$ or 20 GeV, respectively, with some isolation requirements for the muon trigger. To recover possible efficiency losses at high momenta, additional electron and muon triggers which do not make any isolation requirements are included with thresholds of $p_{\mathrm{T}} \geq 60\,\mathrm{GeV}$ and $p_{\mathrm{T}} = 50\,\mathrm{GeV}$, respectively. Candidate events are required to have a primary vertex, defined as the vertex with the highest sum of track p_{T}^2, with at least two associated tracks with $p_{\mathrm{T}} > 400\,\mathrm{MeV}$.

Electron candidates are required to have $p_{\mathrm{T}} > 25\,\mathrm{GeV}$ and to pass "medium" likelihood-based identification requirements [63,64] optimised for the 2015 operating conditions, within the fiducial region of $|\eta| < 2.47$, excluding candidates in the transition region between the barrel and endcap electromagnetic calorimeters, $1.37 < |\eta| < 1.52$. Muons

are reconstructed for $|\eta| < 2.4$ with $p_{\mathrm{T}} > 25$ GeV and must pass "medium" identification requirements [65] also optimised for the 2015 operating conditions. At least one of the lepton candidates is required to match the lepton that triggered the event. The electrons and muons must also satisfy p_{T}-dependent cone-based isolation requirements, using both tracking detector and calorimeter information (described in Refs. [66,67], respectively). The isolation requirements are tuned so that the lepton isolation efficiency is at least 90% for $p_{\mathrm{T}} > 25$ GeV, increasing to 99% at 60 GeV. Both the electron and muon tracks are required to be associated with the primary vertex, using constraints on the transverse impact parameter significance $|d_0|/\Delta d_0$, where d_0 is the transverse impact parameter and Δd_0 is its uncertainty, and on the longitudinal impact parameter z_0 corrected for the reconstructed position of the primary vertex. The transverse impact parameter significance is required to be less than five for electrons and three for muons, while the absolute value of the corrected z_0 multiplied by the sine of the track polar angle is required to be less than 0.5 mm.

Jets of hadrons are reconstructed with the anti-k_t algorithm [68] with radius parameter $R = 0.4$ using topological clusters of energy deposited in the calorimeters [69]. Jets are calibrated using a simulation-based calibration scheme, followed by in situ corrections to account for differences between simulation and data [70]. In order to reduce the effects of pile-up contributions, jets with pseudorapidity $|\eta| < 2.4$ and $p_{\mathrm{T}} < 60$ GeV are required to have a significant fraction of their tracks with an origin compatible with the primary vertex, as defined by the jet vertex tagger algorithm [71]. In addition, the expected average energy contribution from pile-up clusters is subtracted according to the η–ϕ catchment area of the jet [72]. Jets used in the analysis are required to have p_{T} greater than 30 GeV and rapidity $|y| < 2.5$.

The overlap between leptons and jets is removed in a two-step process. The first step removes jets closer than $\Delta R = 0.2$ to a selected electron, and jets closer than $\Delta R = 0.2$ to a selected muon, if they are likely to be reconstructed from photons radiated by the muon. In a second step, electrons and muons are discarded if they are located closer than $\Delta R = 0.4$ to a remaining selected jet. This requirement effectively removes events with leptons and jets which are not reliably simulated in the Monte Carlo simulation.

Events containing a Z-boson candidate are selected by requiring exactly two leptons of the same flavour but of opposite charge with dilepton invariant mass in the range $71 < m_{\ell\ell} < 111$ GeV. The expected and observed numbers of Z-boson candidates selected for each inclusive jet multiplicity, for $N_{\mathrm{jets}} \geq 0 - 7$, are summarised in Table 2, separately for the $Z \to e^+e^-$ and the $Z \to \mu^+\mu^-$ channels. The background evaluation that appears in this table is discussed in Sect. 5. After all requirements, 248,816 and 311,183 $Z+ \geq 1$ jet events are selected in the electron and muon channels, respectively.

4.1 Correction factors and related systematic uncertainties

Some of the object and event selection efficiencies as well as the energy and momentum calibrations modelled by the simulation must be corrected with simulation-to-data correction factors to better match those observed in the data. These corrections and their corresponding uncertainties fall into the following two categories: dependent and not dependent on lepton flavour.

The corrections and uncertainties specific to each leptonic final state ($Z \to e^+e^-$ and $Z \to \mu^+\mu^-$) are as follows:

- **Trigger:** The lepton trigger efficiency is estimated in simulation, with a separate data-driven analysis performed to obtain the simulation-to-data trigger correction factors and their corresponding uncertainties [21].
- **Lepton reconstruction, identification, and isolation:** The lepton selection efficiencies as determined from simulation are also corrected with simulation-to-data correction factors, with corresponding uncertainties [64,65].
- **Energy, momentum scale/resolution:** Uncertainties in the lepton calibrations are estimated [65] because they can cause a change of acceptance because of migration of events across the p_{T} threshold and $m_{\ell\ell}$ boundaries.

The corrections and uncertainties common to the electron and muon final states are as follows:

- **Jet energy scale and resolution**: Uncertainties in the jet energy-scale calibration and resolution have a significant impact on the measurements, especially for the higher jet multiplicities. The jet energy-scale calibration is based on 13 TeV simulation and on in situ corrections obtained from data [70]. The uncertainties are estimated using a decorrelation scheme, resulting in a set of 19 independent parameters which cover all of the relevant calibration uncertainties. The jet energy scale is the dominant systematic uncertainty for all bins with at least one jet. The jet energy-resolution uncertainty is derived by oversmearing the jet energy in the simulation and using the symmetrised variations as the uncertainty.
- **Jet vertex tagger**: The modelling of the output variable from the jet vertex tagger is validated using data events where the Z boson recoils against a jet. A percent-level correction is derived and its statistical and systematic uncertainties are used as additional uncertainties in the efficiency to select jets from the primary vertex [71].
- **Pile-up**: The imperfect modelling of the effects of pile-up leads to acceptance changes at the percent level for different jet multiplicities. To assess this uncertainty, the

Table 2 Fraction of signal and background processes in % in the final selection and expected and observed numbers of events for the various inclusive jet multiplicities considered in the electron (top) and muon (bottom) channels

	+ ≥ 0 jets	+ ≥ 1 jets	+ ≥ 2 jets	+ ≥ 3 jets	+ ≥ 4 jets	+ ≥ 5 jets	+ ≥ 6 jets	+ ≥ 7 jets
Electron channel								
$Z \to e^+e^-$ (%)	99.3	97.6	93.9	90.3	87.3	85.2	83.3	81.2
Top quark (%)	0.2	1.2	3.8	6.5	8.6	9.7	10.5	11.6
Diboson (%)	0.2	0.8	1.6	2.4	3.4	4.4	5.5	6.6
$Z \to \tau^+\tau^-$ (%)	<0.1	<0.1	<0.1	<0.1	<0.1	<0.1	<0.1	<0.1
$W \to e\nu$ (%)	<0.1	<0.1	<0.1	<0.1	<0.1	<0.1	<0.1	<0.1
Multijet (%)	0.2	0.4	0.6	0.7	0.7	0.7	0.7	0.7
Expected	1,327,900	239,500	57,310	14,080	3637	978	252	63
Observed	1,347,900	248,816	59,998	14,377	3587	898	217	48
Muon channel								
$Z \to \mu^+\mu^-$ (%)	99.3	97.5	94.0	90.7	88.3	86.7	84.8	84.6
Top quark (%)	0.2	1.1	3.6	6.0	7.7	8.1	8.7	7.7
Diboson (%)	0.2	0.7	1.6	2.4	3.4	4.5	5.9	7.0
$Z \to \tau^+\tau^-$ (%)	<0.1	<0.1	<0.1	<0.1	<0.1	<0.1	<0.1	<0.1
$W \to \mu\nu$ (%)	<0.1	<0.1	<0.1	<0.1	<0.1	<0.1	<0.1	<0.1
Multijet (%)	0.3	0.6	0.9	0.9	0.7	0.7	0.7	0.7
Expected	1,693,000	300,600	71,230	17,740	4523	1187	307	76
Observed	1,708,602	311,183	74,510	17,865	4387	1081	240	57

average number of interactions per bunch crossing $\langle\mu\rangle$ is varied in simulation so that the behaviour of variables sensitive to pile-up matches that observed in data.

- **Luminosity**: The cross sections have a 2.1% uncertainty from the measurement of the integrated luminosity, which is derived, following a methodology similar to that detailed in Refs. [73,74], from a calibration of the luminosity using x–y beam-separation scans performed in August 2015.

5 Background estimation

Contributions from the electroweak (single boson and diboson) and top-quark (single top-quark and top-quark pair) components of the background are estimated using the Monte Carlo samples described in Sect. 3 with corresponding uncertainties as listed in Table 1. Contributions from multijet events are evaluated with data-driven techniques as described below. A summary of the composition and relative importance of the backgrounds in the candidate Z + jets events is given in Table 2. The overall purity of the Z + jets selections (fraction of signal events in the final selection) ranges from 99% in the inclusive sample to 80–85% in the ≥ 7 jets bin.

5.1 Top-quark and electroweak backgrounds

The dominant contribution to the background at high jet multiplicities comes from $t\bar{t}$ production, with the subsequent leptonic decays of the W bosons originating from the top quarks and is evaluated from simulation. An overall uncertainty of 6%, corresponding to the PDF and scale variations on the theoretical predictions of the inclusive cross sections, is assigned (see Table 1). The $t\bar{t}$ background estimate is validated through a cross-section measurement of $t\bar{t}$ production in the dilepton channel at $\sqrt{s} = 13\,\text{TeV}$ [75] as a function of the jet multiplicity, and the modelling of the additional parton radiation in $t\bar{t}$ events by POWHEG+PY6 was found to be in good agreement with this measurement. In addition, a systematic uncertainty in the modelling of the shape of the distributions is derived by modifying the parton-shower intensity in the nominal simulation sample and by comparing to the predictions from the alternative generator MG5_aMC@NLO+Herwig++ (both listed in Table 1). The small contribution from single-top-quark events is also estimated using POWHEG+PY6 samples and assigned a 6% uncertainty.

Diboson production in leptonic and semileptonic final states with at least two leptons of the same flavour constitutes a co-dominant background for high jet multiplicities (see Table 2). The production of WZ bosons in association with jets at $\sqrt{s} = 13\,\text{TeV}$ was found to be well modelled by

the SHERPA 2.1 generator [76]. A 6% uncertainty, again corresponding to PDF and scale variations on the predictions, is assessed. Since in Ref. [76] the measurement is limited by the statistical precision for dibosons + ≥ 4 jets (resulting in ≥ 6 hadronic jets for semileptonic diboson decays), an additional systematic uncertainty of 50% in the normalisation of the diboson background is added for $Z+ \geq 6$ jets.

Minor background contributions also arise from single-W-boson production decaying to leptonic final states and from single-Z-boson production in the $Z \to \tau^+\tau^-$ process, both estimated with simulation and assigned a 5% uncertainty (as given in Table 1).

5.2 Multijet background

Background-enriched data control regions are used to estimate the multijet contribution in both the electron and muon channels. They are constructed by loosening the lepton identification and isolation requirements. Templates are built from the dilepton invariant mass distribution, a variable that shows discrimination between multijet background and other processes in regions of its kinematic range, but is largely uncorrelated with the variables used to build the multijet control regions. The templates are subsequently normalised to events passing the Z-boson signal selection.

In the electron channel, the multijet templates are built for each jet multiplicity from events with two same-charge leptons with no isolation requirement, whose identification criteria are looser than those of the signal selection, which the leptons must not satisfy. In the muon channel, the control region is similarly built from events with two leptons which are selected with looser identification requirements than the signal selection and also fail the nominal isolation requirement. In both cases, dedicated triggers better suited to this purpose are used to populate the templates. The small electroweak and top-quark contamination is subtracted using simulated events.

The normalisation of the multijet template is estimated with a log-likelihood fit to the measured dilepton invariant mass distribution for the inclusive Z selection, using templates for $Z \to \ell^+\ell^-$ and for the electroweak and top-quark background derived from simulation. The fit is performed in the invariant mass windows of $52 < m_{ee} < 148\,\text{GeV}$ and $40 < m_{\mu\mu} < 80\,\text{GeV}$ for the electron and muon channels, respectively, in order to benefit from the larger multijet contribution in the mass sidebands. The normalisation of the multijet template is allowed to float freely while the remaining non-multijet templates are constrained to be within 6% of the predicted cross sections for these processes as given in Table 1. The multijet fractions are evaluated separately for each jet multiplicity, except for very high jet multiplicities where the templates are statistically limited, and so these fractions are taken from the estimates of the ≥ 5 jets and ≥ 4 jets bins in the electron and muon channels, respectively.

The systematic uncertainties on the multijet background are derived by varying the mass range and bin width of the nominal fit, using the lepton transverse impact parameter d_0 as the fitting variable instead of the invariant mass, using alternative simulation samples for the templates, allowing the normalisations of the non-multijet components to vary independently or within a wider range, and varying the lepton resolution and energy/momentum scales. In addition, given the multiple sources of multijet background in the electron channel, an alternative template is constructed by requiring that the electrons fail to meet an isolation criterion instead of failing to meet the nominal signal selection electron identification criterion.

The resulting estimated multijet fractions in each jet multiplicity bin are given in Table 2. Their corresponding total uncertainties are dominated by their systematic components. These systematic components are approximately 70% of the multijet fraction as estimated in the electron and muon channels.

6 Kinematic distributions

The level of agreement between data and predictions is evaluated from the comparison of kinematic distributions. Figure 1, which presents the dilepton mass for the $Z+ \geq 1$ jet topology and the inclusive jet multiplicity, shows how well the SHERPA 2.2 and MG5_aMC+PY8 CKKWL predictions agree with data. The uncertainty bands shown in these distributions include the statistical uncertainties due to the simulation sample sizes, the event-selection uncertainties described in Sect. 4.1 (omitting the common 2.1% luminosity uncertainty), and the background normalisation uncertainties described in Sect. 5.

7 Unfolding of detector effects

The cross-section measurements presented in this paper are performed within the fiducial acceptance region defined by the following requirements:

- $p_{\text{T}}^{\ell} > 25\,\text{GeV}$, $|\eta^{\ell}| < 2.5$
- $p_{\text{T}}^{\text{jet}} > 30\,\text{GeV}$, $|y^{\text{jet}}| < 2.5$
- $\Delta R(\ell, \text{jet}) > 0.4$
- $71 < m_{\ell\ell} < 111\,\text{GeV}$.

The cross sections are defined at particle ("truth") level, corresponding to dressed electrons and muons from the Z bosons. The particle level also includes jets clustered using

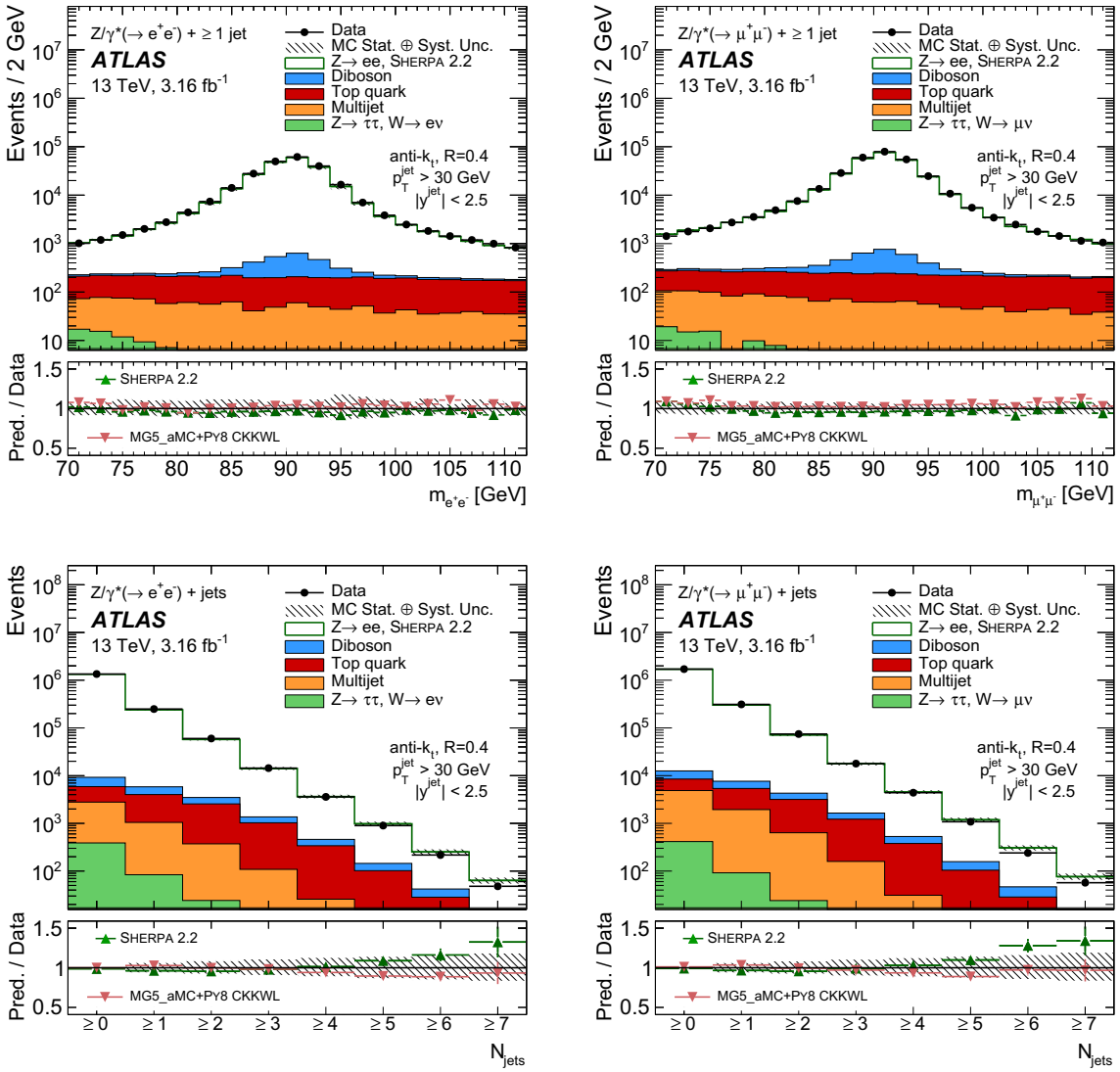

Fig. 1 Dilepton invariant mass for $Z+\geq 1$ jet (*top*) and inclusive jet multiplicity (*bottom*) in the $Z(\rightarrow e^+e^-)+$ jets (*left*) and the $Z(\rightarrow \mu^+\mu^-)+$ jets (*right*) channels. All backgrounds and the signal samples are stacked to produce the figures. Systematic uncertainties for the signal and background distributions are combined in the *hatched band*, and the statistical uncertainty is shown on the *data points*. The uncertainty in the luminosity and the theory uncertainty in the signal prediction are not included in the *uncertainty band*

the anti-k_t algorithm [68] with radius parameter $R = 0.4$ for final-state particles with decay length $c\tau > 10$ mm, excluding the dressed Z-boson decay products.

The fiducial cross sections are estimated from the reconstructed kinematic observables: jet multiplicity, $p_{\mathrm{T}}^{\mathrm{jet}}$ for different jet multiplicities, y^{jet}, $\Delta\phi_{\mathrm{jj}}$, m_{jj}, and H_{T}, for events that pass the selection described in Sect. 4. The expected background components as described in Sect. 5 are subtracted from the distributions in data. A variable-width binning of these observables is used, such that the purity is at least 50% in each bin and the size of the statistical uncertainty in most of the bins remains below 10%.

An iterative Bayesian unfolding technique [77], as implemented in the RooUnfold package [78], is used to unfold the measurements to the particle level, thereby accounting for detector effects related to inefficiencies, resolution, and systematic biases in the central values of the kinematic variables describing both the leptons and the jets. The iterative unfolding technique updates the initial estimators for the generated ("truth") distribution in consecutive steps, using Bayes' theorem in each iteration to derive an unfolding matrix from the initial response matrix (which relates truth and reconstructed distributions of given observables) and the current truth estimator.

The response matrices are constructed using the SHERPA 2.2 $Z(\rightarrow \ell^+\ell^-) +$ jets samples. SHERPA 2.2 is also used to derive the initial truth estimator. In order to enter the response matrix, events must pass the Z-boson selection at generator level and at detector level and contain the number of jets required by the preselection for a given observable at both generator and detector level. Reconstructed jets are required to match the corresponding generator-level jets within a cone of size $\Delta R = 0.4$ for all distributions except global quantities such as the jet multiplicity and H_{T}. A given bin (i, j) in the response matrix therefore corresponds to the probability that a true jet object in bin j is reconstructed in bin i of the distribution. Figure 2 illustrates two examples of response matrices. The resulting ratios of detector-level to truth-level event yields are typically 0.65 and 0.8 for the electron and muon channels, respectively.

The background-subtracted data are corrected for the expected fraction of events with reconstructed objects unmatched to any generator object before entering the iterative unfolding. The number of iterations used for the iterative unfolding of each distribution (two) is chosen by unfolding the SHERPA 2.2 samples reweighted to data and comparing to the generated reweighted distribution. The unfolded event yields are divided by the integrated luminosity of the data sample and the bin width of the distribution in question to provide the final fiducial cross sections. The final result is given by

$$\sigma_i = \frac{1}{\epsilon_i L} \sum_j U_{ij} N_j^{\mathrm{data}} \left(1 - f_j^{\mathrm{unmatched}}\right), \tag{1}$$

where L is the integrated luminosity, ϵ_i is the reconstruction efficiency for truth bin i, N_j^{data} corresponds to the number of events observed in data in reconstructed bin j and $f_j^{\mathrm{unmatched}}$ is its fraction of unmatched events calculated from simulation, and U_{ij} is the unfolding matrix calculated after two iterations, using the updated prior from the first iteration and the response matrix.

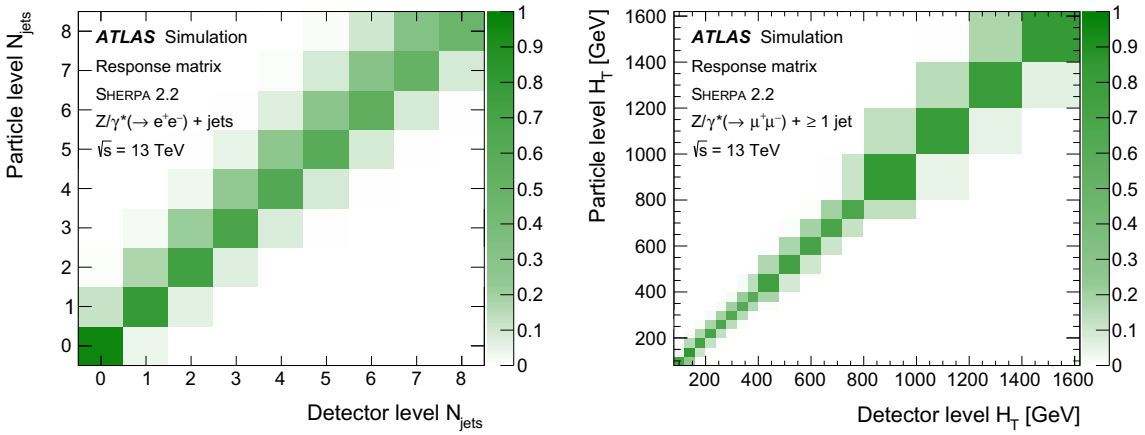

Fig. 2 Response matrices corresponding to the exclusive jet multiplicity for $Z +$ jets events in the electron channel (*left*) and to the H_{T} for $Z+ \geq 1$ jet events in the muon channel (*right*). The sum of the entries in each row is normalised to unity. Both matrices are obtained from SHERPA 2.2

Table 3 Measured fiducial cross sections in the electron and muon channels for successive inclusive jet multiplicities. The total statistical and systematic uncertainties are given, along with the uncertainty in the luminosity

Jet multiplicity	Measured cross section ± (stat.) ± (syst.) ± (lumi.) [pb]							
	$Z \rightarrow ee$				$Z \rightarrow \mu\mu$			
≥0 jets	743±	1±	24±	16	738±	1±	23±	16
≥1 jets	116.6±	0.3±	9.9±	2.5	115.7±	0.2±	9.7±	2.5
≥2 jets	27.1±	0.1±	2.9±	0.6	27.0±	0.1±	2.8±	0.6
≥3 jets	6.20±	0.06±	0.82±	0.14	6.22±	0.05±	0.83±	0.14
≥4 jets	1.49±	0.03±	0.23±	0.04	1.48±	0.03±	0.23±	0.04
≥5 jets	0.357±	0.013±	0.069±	0.009	0.354±	0.012±	0.068±	0.009
≥6 jets	0.082±	0.006±	0.019±	0.002	0.076±	0.005±	0.019±	0.002
≥7 jets	0.0180±	0.0029±	0.0051±	0.0005	0.0166±	0.0027±	0.0060±	0.0004

7.1 Systematic uncertainties associated with the unfolding procedure

The limited size of a simulation sample can create biases in the distributions. Systematic uncertainties account for possible residual biases in the unfolding procedure due to, e.g. modelling of the hadronisation in the simulation, migrations into other kinematic distributions not explicitly part of the unfolding, or the finite bin width used in each distribution. The following uncertainties arise from the unfolding procedure.

- The statistical uncertainties of the response matrices derived from SHERPA 2.2 are propagated to the unfolded cross sections with a toy simulation method. A total of 5000 ensembles (pseudo-experiments) of unfolded samples are generated. For each sample, the number of reconstructed events in each bin is generated randomly according to a Gaussian distribution, where the mean is the nominal number of events before unfolding and the width is its corresponding statistical uncertainty. Unfolding is performed for each ensemble. The widths of resulting distributions are taken as a systematic uncertainty of the unfolding.
- The SHERPA 2.2 samples are reweighted at generator level, such that the distribution of the leading jet p_{T} at detector level matches that observed in the data. The modified SHERPA 2.2 samples are then used to unfold the data again and the variations in the resulting cross sections are used to derive a systematic uncertainty.
- An additional check is performed by unfolding reconstructed MG5_aMC+PY8 CKKWL events using SHERPA 2.2 response matrices. The residual non-closure is accounted for by an additional flat uncertainty of 3% for all distributions.

8 Results

The measured cross sections, presented in Sect. 8.1, are calculated in the electron and muon channels separately and the compatibility of the results of the two channels is evaluated.

Table 4 Relative statistical and systematic uncertainties (in %) in the measured cross sections of Z + jets production for successive inclusive jet multiplicities in the electron (top) and muon (bottom) channels

Systematic source	Relative uncertainty in $\sigma(Z(\to \ell^+\ell^-)+\geq N_{\mathrm{jets}})$ (%)							
	$+\geq 0$ jets	$+\geq 1$ jets	$+\geq 2$ jets	$+\geq 3$ jets	$+\geq 4$ jets	$+\geq 5$ jets	$+\geq 6$ jets	$+\geq 7$ jets
$Z \to e^+e^-$								
Electron trigger	0.1	0.1	0.1	0.2	0.2	0.2	0.3	0.3
Electron selection	1.2	1.6	1.8	1.9	2.3	2.7	2.9	3.8
Jet energy scale	<0.1	6.6	9.2	11.5	13.8	17.3	20.6	23.7
Jet energy resolution	<0.1	3.7	3.7	4.4	5.3	5.2	6.2	7.3
Jet vertex tagger	<0.1	1.3	2.1	2.8	3.6	4.5	5.5	6.3
Pile-up	0.4	0.2	0.1	0.2	0.2	0.1	0.4	0.8
Luminosity	2.1	2.1	2.2	2.3	2.4	2.5	2.6	2.8
Unfolding	3.0	3.0	3.0	3.0	3.0	3.1	3.1	3.2
Background	0.1	0.3	0.6	1.0	1.6	3.3	6.0	11.6
Total syst. Uncertainty	3.9	8.7	11.0	13.4	15.9	19.5	23.6	28.7
Stat. uncertainty	0.1	0.2	0.5	0.9	1.9	3.7	7.7	15.9
$Z \to \mu^+\mu^-$								
Muon trigger	0.4	0.5	0.4	0.5	0.4	0.5	0.9	0.6
Muon selection	0.8	0.9	1.0	1.0	1.0	1.5	4.2	16.6
Jet energy scale	<0.1	6.8	9.1	11.9	14.0	17.0	20.9	23.7
Jet energy resolution	<0.1	3.6	3.6	4.1	5.0	5.9	6.2	9.3
Jet vertex tagger	<0.1	1.3	2.1	3.1	3.6	4.4	5.6	6.6
Pile-up	0.4	0.1	<0.1	0.3	0.5	0.1	0.4	0.9
Luminosity	2.1	2.1	2.2	2.3	2.4	2.5	2.6	2.7
Unfolding	3.0	3.0	3.0	3.0	3.0	3.1	3.1	3.2
Background	0.2	0.4	0.6	0.9	1.7	4.0	7.4	12.9
Total syst. Uncertainty	3.8	8.7	10.8	13.6	16.0	19.4	24.6	36.3
Stat. uncertainty	0.1	0.2	0.4	0.8	1.7	3.4	7.2	16.3

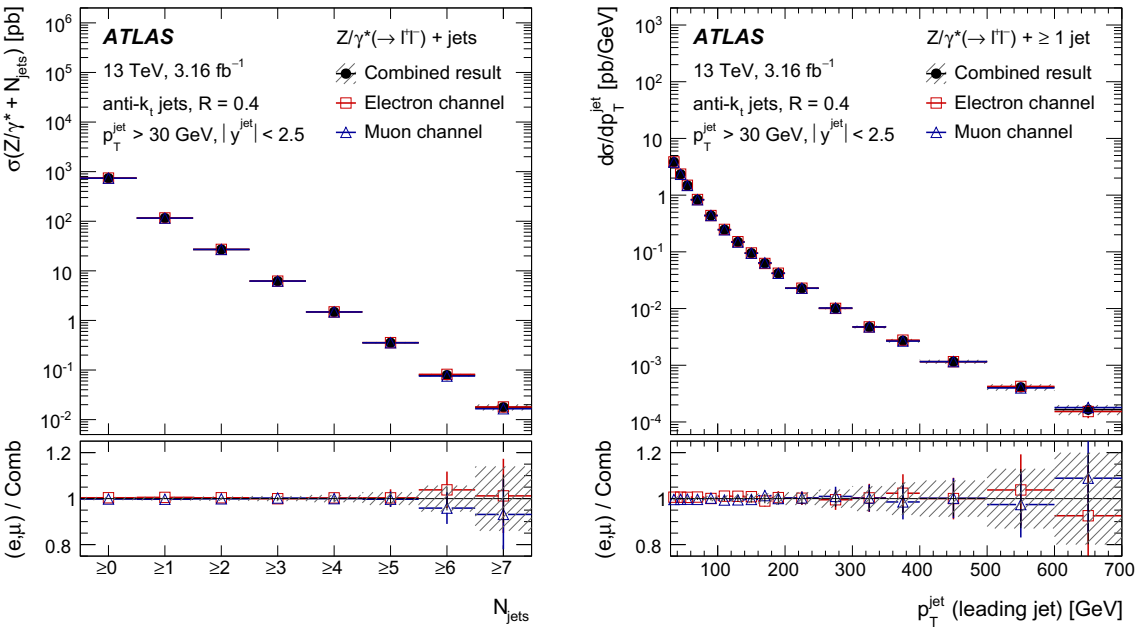

Fig. 3 Measured fiducial cross section as a function of the inclusive jet multiplicity (*left*) and the leading jet p_{T} for inclusive $Z+\geq 1$ jet events (*right*) in the electron and the muon channels and compared to their combined value. The ratios of the two measurements to the combined results are also shown in the *bottom panels*. The *error bars* indicate the statistical uncertainty, and the *hatched bands* the statistical and the flavour-uncorrelated systematic uncertainties of the combined result, added in quadrature

Table 5 Measured combined fiducial cross sections for successive inclusive jet multiplicities. The statistical, systematic, and luminosity uncertainties are given

Jet multiplicity	Measured cross section $\pm$(stat.) $\pm$(syst.) $\pm$(lumi.) [pb] $Z \to \ell\ell$
$\geq$0 jets	740 $\pm$ 1 $\pm$ 23 $\pm$ 16
$\geq$1 jets	116.0 $\pm$ 0.3 $\pm$ 9.7 $\pm$ 2.5
$\geq$2 jets	27.0 $\pm$ 0.1 $\pm$ 2.8 $\pm$ 0.6
$\geq$3 jets	6.20 $\pm$ 0.04 $\pm$ 0.82 $\pm$ 0.14
$\geq$4 jets	1.48 $\pm$ 0.02 $\pm$ 0.23 $\pm$ 0.04
$\geq$5 jets	0.36 $\pm$ 0.01 $\pm$ 0.07 $\pm$ 0.01
$\geq$6 jets	0.079 $\pm$ 0.004 $\pm$ 0.018 $\pm$ 0.002
$\geq$7 jets	0.0178 $\pm$ 0.0019 $\pm$ 0.0049 $\pm$ 0.0005

Table 6 Measured combined ratios of the fiducial cross sections for successive inclusive jet multiplicities. The statistical, systematic, and luminosity uncertainties are given

Jet multiplicity	Measured cross-section ratio $\pm$(stat.) $\pm$(syst.) $\pm$(lumi.) $Z \to \ell\ell$
$\geq$1 jets/$\geq$0 jets	0.1568 $\pm$ 0.0004 $\pm$ 0.0131 $\pm$ 0.0001
$\geq$2 jets/$\geq$1 jets	0.2327 $\pm$ 0.0011 $\pm$ 0.0093 $\pm$ 0.0002
$\geq$3 jets/$\geq$2 jets	0.2299 $\pm$ 0.0018 $\pm$ 0.0095 $\pm$ 0.0002
$\geq$4 jets/$\geq$3 jets	0.2390 $\pm$ 0.0035 $\pm$ 0.0094 $\pm$ 0.0002
$\geq$5 jets/$\geq$4 jets	0.2397 $\pm$ 0.0068 $\pm$ 0.0111 $\pm$ 0.0002
$\geq$6 jets/$\geq$5 jets	0.2213 $\pm$ 0.0127 $\pm$ 0.0123 $\pm$ 0.0003
$\geq$7 jets/$\geq$6 jets	0.2240 $\pm$ 0.0264 $\pm$ 0.0222 $\pm$ 0.0003

In order to improve the precision of the measurement, these results are then combined, taking into account the correlations of the systematic uncertainties. The comparisons of the combined results to the predictions are presented in Sect. 8.2.

8.1 Results in the individual channels and the combination

The fiducial cross-section measurements in the $Z(\to e^+e^-)+$ jets and $Z(\to \mu^+\mu^-)+$ jets channels as a function of the inclusive jet multiplicities are presented in Table 3. The data statistical uncertainties are propagated through the unfolding by using pseudo-experiments. As mentioned in Sect. 7, the systematic uncertainties are propagated through the unfolding via the migration matrices and via the variation of the subtracted background. Table 4 shows the resulting total relative statistical and systematic uncertainties as well as the systematic components [lepton trigger, lepton selection, jet energy scale and resolution, jet vertex tagging, pile-up, luminosity (all described in Sect. 4.1)], unfolding (described in Sect. 7), and background (described in Sect. 5) as a function of the inclusive jet multiplicity, presented separately for the electron and muon channels. The jet energy scale is the

dominant systematic uncertainty for all bins with at least one jet.

Figure 3 shows a comparison of the electron and muon channels for the measured fiducial cross section as a function of the inclusive jet multiplicity and of the leading jet p_{T} for inclusive $Z+ \geq 1$ jet events. This figure demonstrates that the results in the electron and muon channels are compatible and hence can be combined to improve the precision of the measurement. This figure also shows the result of this combination described below.

The results from the electron and muon channels are combined at dressed level for each distribution separately: inclusive and exclusive jet multiplicities, ratio for successive inclusive jet multiplicities, leading jet p_{T} for $Z+ \geq 1, 2, 3, 4$ jet events and jet p_{T} for exclusive $Z + 1$ jet events, leading jet rapidity for inclusive $Z+ \geq 1$ jet events, H_{T}, $\Delta\phi_{\mathrm{jj}}$, and m_{jj}. A χ^2 function whose sum runs over all measurement sets (electrons and muons), measurement points, and some of the uncertainty sources, is used for the combination [79,80] and distinguishes between bin-to-bin correlated and uncorrelated sources of uncertainties, the latter comprising the statistical uncertainty of the data and the statistical unfolding uncertainty. Uncertainties specific to the lepton flavour and to the background are included in the χ^2 function, while the remaining, flavour-uncorrelated, systematic uncertainties related to jets, pile-up, luminosity, and unfolding are averaged after the combination.

8.2 Comparisons of results to predictions

The cross-section measurement for different inclusive $Z +$ jets multiplicities and their ratios obtained from the combination are found in Tables 5 and 6. Figure 4 shows the comparison of these results with the NLO QCD fixed-order calculations from BlackHat+Sherpa and with the predictions from Sherpa 2.2, Alpgen+Py6, MG5_aMC+Py8 CKKWL, and MG5_aMC+Py8 FxFx. The plots show the particle-level cross section with the generator predictions normalised to the inclusive NNLO cross sections in the top panel, accompanied by the ratios of the various predictions with respect to the data in the bottom panels. Uncertainties from the parton distribution functions and QCD scale variations are included in the BlackHat+Sherpa predictions, as described in Sect. 3.3. A constant 5% theoretical uncertainty is used for Sherpa 2.2, Alpgen+Py6, MG5_aMC+Py8 CKKWL, and MG5_aMC+Py8 FxFx, as described in Table 1. The

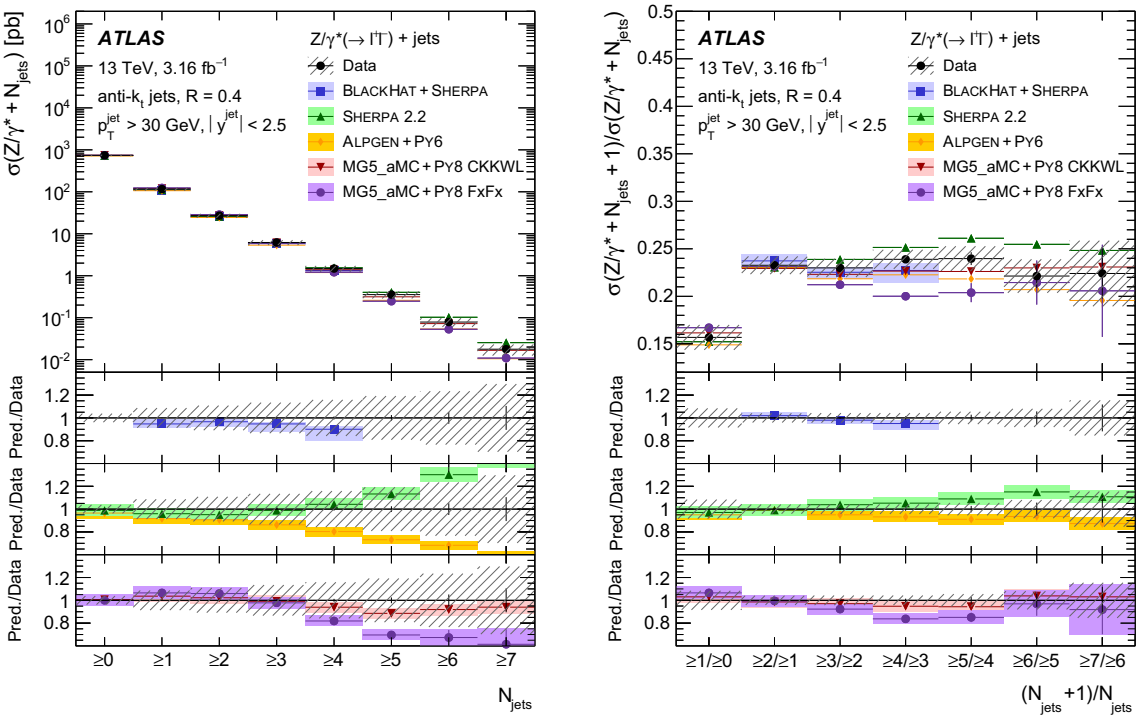

Fig. 4 Measured cross section as a function of the inclusive jet multiplicity (*left*) and ratio for successive inclusive jet multiplicities (*right*) for inclusive $Z +$ jets events. The data are compared to the predictions from BlackHat+Sherpa, Sherpa 2.2, Alpgen+Py6, MG5_aMC+Py8 CKKWL, and MG5_aMC+Py8 FxFx. The *error bars* correspond to the statistical uncertainty, and the *hatched bands* to the data statistical and systematic uncertainties (including luminosity) added in quadrature. A constant 5% theoretical uncertainty is used for Sherpa 2.2, Alpgen+Py6, MG5_aMC+Py8 CKKWL, and MG5_aMC+Py8 FxFx. Uncertainties from the parton distribution functions and QCD scale variations are included in the BlackHat+Sherpa predictions, as described in Sect. 3.3

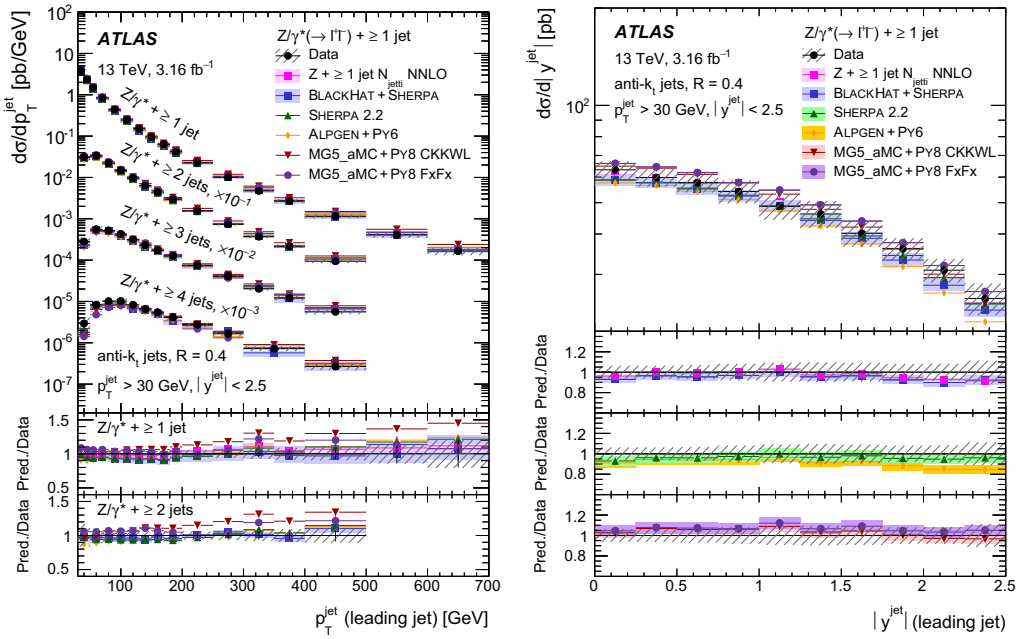

Fig. 5 Measured cross section as a function of the leading jet p_T for inclusive $Z+ \geq 1, 2, 3, 4$ jet events (*left*) and absolute value of the leading jet rapidity for inclusive $Z+ \geq 1$ jet events (*right*). The data are compared to the predictions from $Z+ \geq 1$ jet N_{jetti} NNLO, BLACKHAT+SHERPA, SHERPA 2.2, ALPGEN+PY6, MG5_aMC+PY8 CKKWL, and MG5_aMC+PY8 FxFx. The *error bars* correspond to the statistical uncertainty, and the *hatched bands* to the data statistical and systematic uncertainties (including luminosity) added in quadrature. The details of the prediction uncertainties are given in the text. For clarity, *uncertainty bands* are not shown for the Monte Carlo predictions in the *left-hand plot*. Uncertainties from the QCD scale variations for the $Z+ \geq 1$ jet N_{jetti} NNLO predictions are included, as described in Sect. 3.3

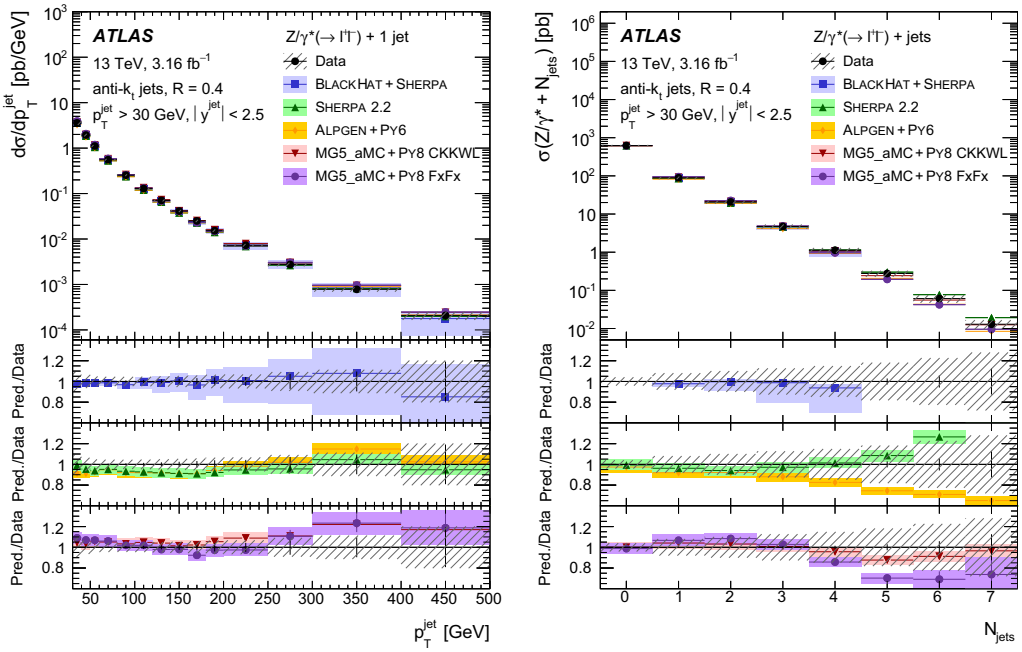

Fig. 6 Measured cross section as a function of jet p_T for exclusive $Z+1$ jet events (*left*) and exclusive jet multiplicity (*right*). The data are compared to the predictions from BLACKHAT+SHERPA, SHERPA 2.2, ALPGEN+PY6, MG5_aMC+PY8 CKKWL, and MG5_aMC+PY8 FxFx. The *error bars* correspond to the statistical uncertainty, and the *hatched bands* to the data statistical and systematic uncertainties (including luminosity) added in quadrature. The details of the prediction uncertainties are given in the text

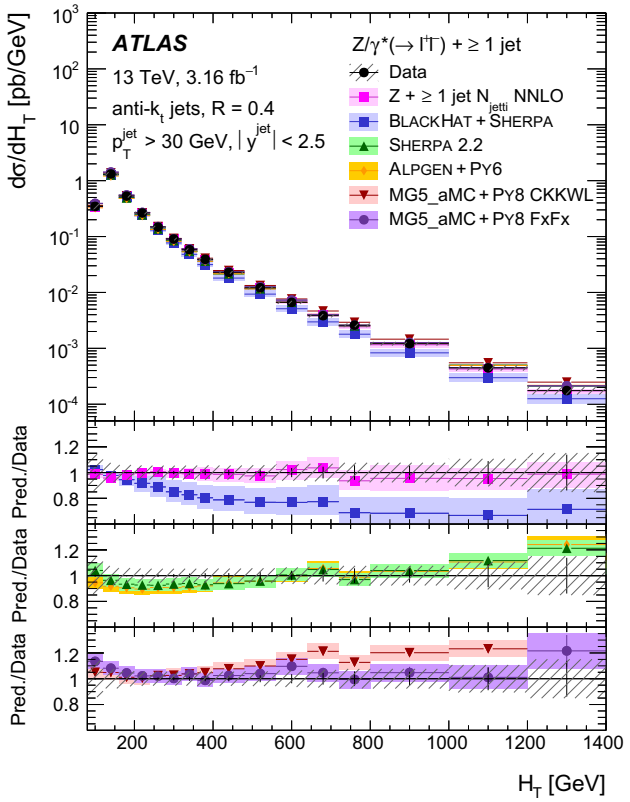

Fig. 7 Measured cross section as a function of H_{T} for inclusive $Z+ \geq 1$ jet events. The data are compared to the predictions from $Z+ \geq 1$ jet $\mathrm{N_{jetti}}$ NNLO, BLACKHAT+SHERPA, SHERPA 2.2, ALPGEN+PY6, MG5_aMC+PY8 CKKWL, and MG5_aMC+PY8 FxFx. The *error bars* correspond to the statistical uncertainty, and the *hatched bands* to the data statistical and systematic uncertainties (including luminosity) added in quadrature. The details of the prediction uncertainties are given in the text

inclusive jet multiplicity decreases logarithmically while the ratio is flat in the presence of at least one jet. The predictions are in agreement with the observed cross sections and their ratios, except for SHERPA 2.2, ALPGEN+PY6 and MG5_aMC+PY8 FxFx for high jet multiplicity, where a non-negligible fraction of the jets are produced by the parton shower.

The jet transverse momentum is a fundamental observable of the Z + jets process and probes pQCD over a wide range of scales. Moreover, understanding the kinematics of jets in events with vector bosons associated with several jets is essential for the modelling of backgrounds for other SM processes and searches beyond the SM. The leading jet p_{T} distribution (which is correlated with the p_{T} of the Z boson) in inclusive $Z+ \geq 1, 2, 3, 4$ jet events is shown in Fig. 5 and ranges up to 700 GeV. The LO generator MG5_aMC+PY8 CKKWL models a too-hard jet p_{T} spectrum. This feature is known from studies of LO generators in pp collisions at lower centre-of-mass energies [11], and can be interpreted as an indication that the dynamic factorisation and renormalisation scale used in the generation is not appropriate for the full jet p_{T} range. In contrast, the predictions from BLACKHAT+SHERPA, SHERPA 2.2, and MG5_aMC+PY8 FxFx, which are based on NLO matrix elements, are in agreement with the measured cross section within the systematic uncertainties over the full leading jet p_{T} range. ALPGEN+PY6 also shows good agreement with the measured data. The $Z+ \geq 1$ jet $\mathrm{N_{jetti}}$ NNLO prediction models the spectrum for the $Z+ \geq 1$ jet events well. Uncertainties from the QCD scale variations for the $Z+ \geq 1$ jet $\mathrm{N_{jetti}}$ NNLO predictions are included in the uncertainty band, as described in Sect. 3.3. For the leading jet rapidity distribution in inclusive $Z+ \geq 1$ jet events, also shown in this figure, all predictions show good agreement with the measured data within the uncertainties.

The exclusive jet p_{T} distribution probes the validity of $Z + 1$ jet predictions at increasing QCD scales represented by the jet p_{T} in the presence of a jet veto at a constant low scale; for a jet p_{T} range of several hundred GeV, accessible with the current data set, the jet scale is of order ten times larger than the veto scale (30 GeV). Figure 6 demonstrates that all predictions studied are consistent with the data within systematic uncertainties over the full jet p_{T} range (up to 500 GeV). This figure also shows the measured cross section as a function of the exclusive jet multiplicity, which decreases logarithmically. Similar trends as for the inclusive jet multiplicity (Fig. 4) are observed.

Quantities based on inclusive p_{T} sums of final-state objects, such as H_{T}, the scalar p_{T} sum of all visible objects in the final state, are often employed in searches for physics beyond the Standard Model, to enrich final states resulting from the decay of heavy particles. The values H_{T} or $H_{\mathrm{T}}/2$ are also commonly used choices for scales for higher-order perturbative QCD calculations. Large values for this quantity can result either from a small number of very energetic particles or from a large number of less energetic particles. Figure 7 shows the measured cross sections as a function of the H_{T} distribution (up to 1400 GeV) in inclusive $Z+ \geq 1$ jet events. The predictions from SHERPA 2.2, ALPGEN+PY6 and MG5_aMC+PY8 FxFx describe well the H_{T} distribution. The prediction from MG5_aMC+PY8 CKKWL describes well the turn-over in the softer part of the H_{T} spectrum, but overestimates the contribution at large values of H_{T}, in line with the overestimate of the cross sections for hard jets. The fixed-order $Z+ \geq 1$ jet prediction from BLACKHAT+SHERPA underestimates the cross section for values of $H_{\mathrm{T}} > 300$ GeV, as observed in similar measurements at lower centre-of-mass energies [11,81], due to the missing contributions from events with higher parton multiplicities, which for large values of H_{T} constitute a substantial portion of the data. Agreement is recovered by adding higher orders

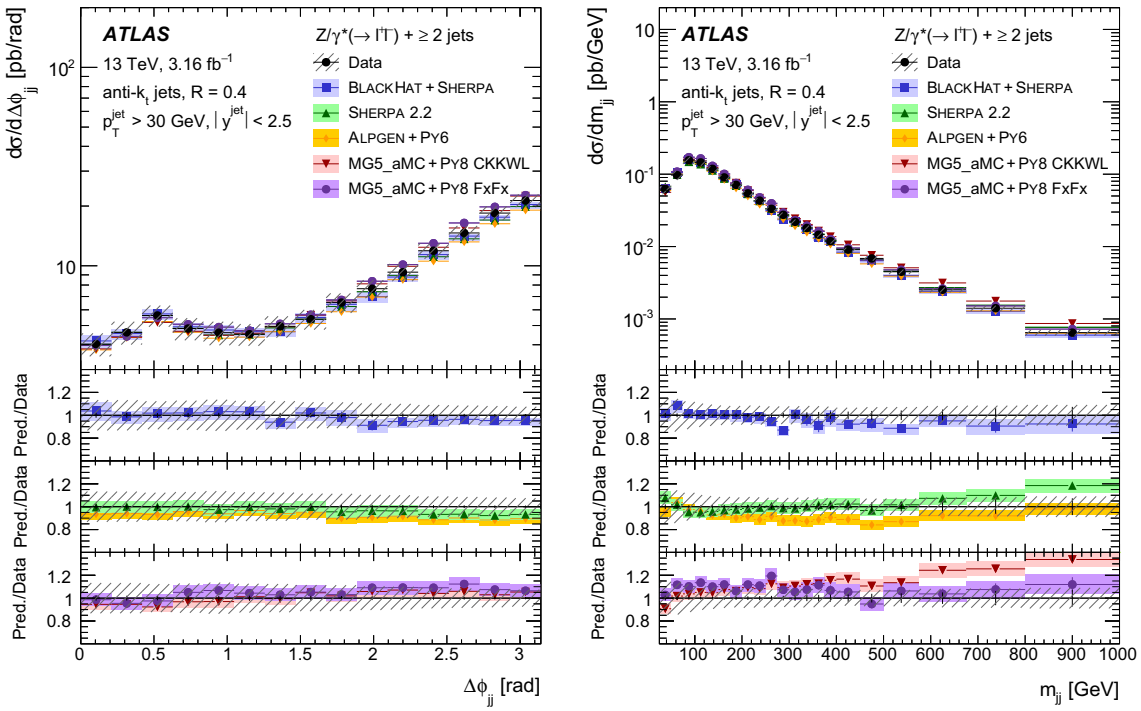

Fig. 8 Measured cross section as a function of $\Delta\phi_{\mathrm{jj}}$ (*left*) and m_{jj} (*right*) for inclusive $Z+\geq 2$ jet events. The data are compared to the predictions from BLACKHAT+SHERPA, SHERPA 2.2, ALPGEN+PY6, MG5_aMC+PY8 CKKWL, and MG5_aMC+PY8 FxFx. The *error bars* correspond to the statistical uncertainty, and the *hatched bands* to the data statistical and systematic uncertainties (including luminosity) added in quadrature. The details of the prediction uncertainties are given in the text

in perturbative QCD, as demonstrated by the good description of H_{T} by $Z+\geq 1$ jet $\mathrm{N_{jetti}}$ NNLO.

Angular relations between the two leading jets and the dijet mass are frequently used to separate either heavier SM particles or beyond-SM physics from the $Z+$ jets process. Figure 8 shows the differential cross section as a function of azimuthal angular difference between the two leading jets for $Z+\geq 2$ jet events, $\Delta\phi_{\mathrm{jj}}$. The tendency of the two jets to be back-to-back in the transverse plane is well modelled by all predictions. This figure also shows the measured cross sections as a function of the invariant mass m_{jj} of the two leading jets for $Z+\geq 2$ jet events. The shape of the dijet mass is modelled well by BLACKHAT+SHERPA, SHERPA 2.2, ALPGEN+PY6, and MG5_aMC+PY8 FxFx, whereas MG5_aMC+PY8 CKKWL shows a harder spectrum.

9 Conclusion

Proton–proton collision data at $\sqrt{s}=13\,\mathrm{TeV}$ from the LHC, corresponding to a total integrated luminosity of $3.16\,\mathrm{fb}^{-1}$, have been analysed by the ATLAS collaboration to study events with Z bosons decaying to electron or muon pairs, produced in association with one or more jets. The fiducial production cross sections for $Z+\geq 0$–7 jets have been measured, within the acceptance region defined by $p_{\mathrm{T}}^{\ell}>25\,\mathrm{GeV}$, $|\eta^{\ell}|<2.5$, $71<m_{\ell\ell}<111\,\mathrm{GeV}$, $p_{\mathrm{T}}^{\mathrm{jet}}>30\,\mathrm{GeV}$, $|y^{\mathrm{jet}}|<2.5$, and $\Delta R(\ell,\mathrm{jet})>0.4$, with a precision ranging from 4 to 30%. Ratios of cross sections for successive jet multiplicities and cross-section measurements as a function of different key variables such as the jet multiplicities, jet p_{T} for exclusive $Z+1$ jet events, leading jet p_{T} for $Z+\geq 1, 2, 3, 4$ jet events, leading jet rapidity for $Z+\geq 1$ jet events, H_{T}, $\Delta\phi_{\mathrm{jj}}$ and m_{jj} have also been derived.

The measurements have been compared to fixed-order calculations at NLO from BLACKHAT+SHERPA and at NNLO from the $Z+\geq 1$ jet $\mathrm{N_{jetti}}$ NNLO calculation, and to predictions from the generators SHERPA 2.2, ALPGEN+PY6, MG5_aMC+PY8 CKKWL, and MG5_aMC+PY8 FxFx. In general, the predictions are in good agreement with the observed cross sections and cross-section ratios within the uncertainties. Distributions which are dominated by a single jet multiplicity are modelled well by fixed-order NLO calculations, even in the presence of a jet veto at a low scale. The ME+PS generator MG5_aMC+PY8 CKKWL, which is based on LO matrix elements, models a too-hard jet spectrum, as observed in $\sqrt{s}=7\,\mathrm{TeV}$ pp collisions. It however models well the inclusive jet multiplicity distribution over the full multiplicity range. The modelling of the jet p_{T} and related

observables is significantly improved by the ME+PS@NLO generators SHERPA 2.2 and MG5_aMC+PY8 FxFx, which use NLO matrix elements for up to two additional partons. The recent $Z+ \geq 1$ jet N_{jetti} NNLO predictions describe well key distributions such as the leading jet p_T and H_T. The results presented in this paper provide essential input for the further optimisation of the Monte Carlo generators of Z+ jets production and constitute a powerful test of perturbative QCD for processes with a higher number of partons in the final state.

Acknowledgements We thank CERN for the very successful operation of the LHC, as well as the support staff from our institutions without whom ATLAS could not be operated efficiently. We acknowledge the support of ANPCyT, Argentina; YerPhI, Armenia; ARC, Australia; BMWFW and FWF, Austria; ANAS, Azerbaijan; SSTC, Belarus; CNPq and FAPESP, Brazil; NSERC, NRC and CFI, Canada; CERN; CONICYT, Chile; CAS, MOST and NSFC, China; COLCIENCIAS, Colombia; MSMT CR, MPO CR and VSC CR, Czech Republic; DNRF and DNSRC, Denmark; IN2P3-CNRS, CEA-DSM/IRFU, France; SRNSF, Georgia; BMBF, HGF, and MPG, Germany; GSRT, Greece; RGC, Hong Kong SAR, China; ISF, I-CORE and Benoziyo Center, Israel; INFN, Italy; MEXT and JSPS, Japan; CNRST, Morocco; NWO, Netherlands; RCN, Norway; MNiSW and NCN, Poland; FCT, Portugal; MNE/IFA, Romania; MES of Russia and NRC KI, Russian Federation; JINR; MESTD, Serbia; MSSR, Slovakia; ARRS and MIZŠ, Slovenia; DST/NRF, South Africa; MINECO, Spain; SRC and Wallenberg Foundation, Sweden; SERI, SNSF and Cantons of Bern and Geneva, Switzerland; MOST, Taiwan; TAEK, Turkey; STFC, United Kingdom; DOE and NSF, United States of America. In addition, individual groups and members have received support from BCKDF, the Canada Council, CANARIE, CRC, Compute Canada, FQRNT, and the Ontario Innovation Trust, Canada; EPLANET, ERC, ERDF, FP7, Horizon 2020 and Marie Skłodowska-Curie Actions, European Union; Investissements d'Avenir Labex and Idex, ANR, Région Auvergne and Fondation Partager le Savoir, France; DFG and AvH Foundation, Germany; Herakleitos, Thales and Aristeia programmes co-financed by EU-ESF and the Greek NSRF; BSF, GIF and Minerva, Israel; BRF, Norway; CERCA Programme Generalitat de Catalunya, Generalitat Valenciana, Spain; the Royal Society and Leverhulme Trust, United Kingdom. The crucial computing support from all WLCG partners is acknowledged gratefully, in particular from CERN, the ATLAS Tier-1 facilities at TRIUMF (Canada), NDGF (Denmark, Norway, Sweden), CC-IN2P3 (France), KIT/GridKA (Germany), INFN-CNAF (Italy), NL-T1 (Netherlands), PIC (Spain), ASGC (Taiwan), RAL (UK) and BNL (USA), the Tier-2 facilities worldwide and large non-WLCG resource providers. Major contributors of computing resources are listed in Ref. [82].

Open Access This article is distributed under the terms of the Creative Commons Attribution 4.0 International License (http://creativecommons.org/licenses/by/4.0/), which permits unrestricted use, distribution, and reproduction in any medium, provided you give appropriate credit to the original author(s) and the source, provide a link to the Creative Commons license, and indicate if changes were made.
Funded by SCOAP[3].

References

1. D.J. Gross, F. Wilczek, Asymptotically free Gauge theories. Phys. Rev. D **8**, 3633 (1973). doi:10.1103/PhysRevD.8.3633
2. H.D. Politzer, Asymptotic freedom: an approach to strong interactions. Phys. Rep. **14**, 129 (1974). doi:10.1016/0370-1573(74)90014-3
3. R. Boughezal et al., Z-boson production in association with a jet at next-to-next-to-leading order in perturbative QCD. Phys. Rev. Lett. **116**, 152001 (2016). doi:10.1103/PhysRevLett.116.152001. arXiv:1512.01291 [hep-ph]
4. R. Boughezal, X. Liu, F. Petriello, Phenomenology of the Z-boson plus jet process at NNLO. Phys. Rev. D **94**, 074015 (2016). doi:10.1103/PhysRevD.94.074015. arXiv:1602.08140 [hep-ph]
5. A. Gehrmann-De Ridder, T. Gehrmann, E.W.N. Glover, A. Huss, T.A. Morgan, Precise QCD predictions for the production of a Z boson in association with a hadronic jet. Phys. Rev. Lett. **117**, 022001 (2016). doi:10.1103/PhysRevLett.117.022001. arXiv:1507.02850 [hep-ph]
6. A. Gehrmann-De Ridder, T. Gehrmann, E.W.N. Glover, A. Huss, T.A. Morgan, The NNLO QCD corrections to Z boson production at large transverse momentum. JHEP **07**, 133 (2016). doi:10.1007/JHEP07(2016)133. arXiv:1605.04295 [hep-ph]
7. ATLAS Collaboration, The ATLAS Experiment at the CERN Large Hadron Collider. JINST **3**, S08003 (2008). doi:10.1088/1748-0221/3/08/S08003
8. CMS Collaboration, The CMS experiment at the CERN LHC. JINST **3**, S08004 (2008). doi:10.1088/1748-0221/3/08/S08004
9. LHCb Collaboration, The LHCb detector at the LHC. JINST **3**, S08005 (2008). doi:10.1088/1748-0221/3/08/S08005
10. L. Evans, P. Bryant, LHC Machine, JINST **3**, S08001 (2008). doi:10.1088/1748-0221/3/08/S08001
11. ATLAS Collaboration, Measurement of the production cross section of jets in association with a Z boson in pp collisions at $\sqrt{s} = 7$ TeV with the ATLAS detector. JHEP **07**, 032 (2013). doi:10.1007/JHEP07(2013)032. arXiv:1304.7098 [hep-ex]
12. CMS Collaboration, Rapidity distributions in exclusive Z + jet and γ + jet events in pp collisions at $\sqrt{s} = 7$ TeV. Phys. Rev. D **88**, 112009 (2013). doi:10.1103/PhysRevD.88.112009. arXiv:1310.3082 [hep-ex]
13. CMS Collaboration, Event shapes and azimuthal correlations in Z + jets events in pp collisions at $\sqrt{s} = 7$ TeV. Phys. Lett. B **722**, 238 (2013). doi:10.1016/j.physletb.2013.04.025. arXiv:1301.1646 [hep-ex]
14. CMS Collaboration, Measurements of jet multiplicity and differential production cross sections of $Z+$ jets events in proton-proton collisions at $\sqrt{s} = 7$ TeV. Phys. Rev. D **91**, 052008 (2015). doi:10.1103/PhysRevD.91.052008. arXiv:1408.3104 [hep-ex]
15. LHCb Collaboration, Study of forward Z + jet production in pp collisions at $\sqrt{s} = 7$ TeV. JHEP **01**, 033 (2014). doi:10.1007/JHEP01(2014)033. arXiv:1310.8197 [hep-ex]
16. CMS Collaboration, Comparison of the Z/γ^* + jets to γ + jets cross sections in pp collisions at $\sqrt{s} = 8$ TeV. JHEP **10**, 128 (2015). doi:10.1007/JHEP04(2016)010, doi:10.1007/JHEP10(2015)128, arXiv:1505.06520 [hep-ex] [Erratum: JHEP 04 (2016) 010]
17. CMS Collaboration, Measurements of the differential production cross sections for a Z boson in association with jets in pp collisions at $\sqrt{s} = 8$ TeV (2016). arXiv:1611.03844 [hep-ex]
18. LHCb Collaboration, Measurement of forward W and Z boson production in association with jets in proton-proton collisions at $\sqrt{s} =$ 8 TeV. JHEP **05**, 131 (2016). doi:10.1007/JHEP05(2016)131. arXiv:1605.00951 [hep-ex]
19. T.A. Aaltonen et al., Measurement of differential production cross section for Z/γ^* bosons in association with jets in $p\bar{p}$ collisions at $\sqrt{s} = 1.96$ TeV. Phys. Rev. D **91**, 012002 (2015). doi:10.1103/PhysRevD.91.012002. arXiv:1409.4359 [hep-ex]
20. V.M. Abazov et al., Measurement of $Z/\gamma*$+jet+X angular distributions in p anti-p collisions at $\sqrt{s} = 1.96$ TeV. Phys. Lett. B **682**, 370 (2010). doi:10.1016/j.physletb.2009.11.012. arXiv:0907.4286 [hep-ex]

21. ATLAS Collaboration, Performance of the ATLAS trigger system in 2015 (2016). arXiv:1611.09661 [hep-ex]
22. S. Agostinelli et al., GEANT4: a simulation toolkit. Nucl. Instrum. Meth. A **506**, 250 (2003). doi:10.1016/S0168-9002(03)01368-8
23. ATLAS Collaboration, The ATLAS simulation infrastructure. Eur. Phys. J. C **70**, 823 (2010). doi:10.1140/epjc/s10052-010-1429-9, arXiv:1005.4568 [hep-ex]
24. C. Anastasiou, L.J. Dixon, K. Melnikov, F. Petriello, High precision QCD at hadron colliders: electroweak gauge boson rapidity distributions at NNLO. Phys. Rev. D **69**, 094008 (2004). doi:10.1103/PhysRevD.69.094008. arXiv:hep-ph/0312266
25. R. Gavin et al., FEWZ 2.0: a code for hadronic Z production at next-to-next-to-leading order. Comput. Phys. Commun. **182**, 2388 (2011). doi:10.1016/j.cpc.2011.06.008. arXiv:1011.3540 [hep-ph]
26. R. Gavin et al., W physics at the LHC with FEWZ 2.1. Comput. Phys. Commun. **184**, 208 (2013). doi:10.1016/j.cpc.2012.09.005. arXiv:1201.5896 [hep-ph]
27. Y. Li, F. Petriello, Combining QCD and electroweak corrections to dilepton production in FEWZ. Phys. Rev. D **86**, 094034 (2012). doi:10.1103/PhysRevD.86.094034. arXiv:1208.5967 [hep-ph]
28. M. Czakon, A. Mitov, Top++: a program for the calculation of the top-pair cross-section at Hadron colliders. Comput. Phys. Commun. **185**, 2930 (2014). doi:10.1016/j.cpc.2014.06.021. arXiv:1112.5675 [hep-ph]
29. N. Kidonakis, Two-loop soft anomalous dimensions for single top quark associated production with a W^- or H^-. Phys. Rev. D **82**, 054018 (2010). doi:10.1103/PhysRevD.82.054018. arXiv:1005.4451 [hep-ph]
30. N. Kidonakis, Next-to-next-to-leading-order collinear and soft gluon corrections for t-channel single top quark production. Phys. Rev. D **83**, 091503 (2011). doi:10.1103/PhysRevD.83.091503. arXiv:1103.2792 [hep-ph]
31. T. Gleisberg et al., Event generation with SHERPA 1.1. JHEP **02**, 007 (2009). doi:10.1088/1126-6708/2009/02/007. arXiv:0811.4622 [hep-ph]
32. M. Grazzini et al., $W^{\pm}Z$ production at hadron colliders in NNLO QCD. Phys. Lett. B **761**, 179 (2016). doi:10.1016/j.physletb.2016.08.017. arXiv:1604.08576 [hep-ph]
33. T. Gehrmann et al., W^+W^- Production at Hadron colliders in next to next to leading order QCD. Phys. Rev. Lett. **113**, 212001 (2014). doi:10.1103/PhysRevLett.113.212001. arXiv:1408.5243 [hep-ph]
34. T. Gleisberg, S. Höche, Comix, a new matrix element generator. JHEP **12**, 039 (2008). doi:10.1088/1126-6708/2008/12/039. arXiv:0808.3674 [hep-ph]
35. F. Cascioli, P. Maierhofer, S. Pozzorini, Scattering amplitudes with open loops. Phys. Rev. Lett. **108**, 111601 (2012). doi:10.1103/PhysRevLett.108.111601. arXiv:1111.5206 [hep-ph]
36. S. Schumann, F. Krauss, A Parton shower algorithm based on Catani-Seymour dipole factorisation. JHEP **03**, 038 (2008). doi:10.1088/1126-6708/2008/03/038. arXiv:0709.1027 [hep-ph]
37. S. Höche, F. Krauss, M. Schönherr, F. Siegert, QCD matrix elements + parton showers: the NLO case. JHEP **04**, 027 (2013). doi:10.1007/JHEP04(2013)027. arXiv:1207.5030 [hep-ph]
38. R.D. Ball et al., Parton distributions for the LHC Run II. JHEP **04**, 040 (2015). doi:10.1007/JHEP04(2015)040. arXiv:1410.8849 [hep-ph]
39. J. Alwall et al., The automated computation of tree-level and next-to-leading order differential cross sections, and their matching to parton shower simulations. JHEP **07**, 079 (2014). doi:10.1007/JHEP07(2014)079. arXiv:1405.0301 [hep-ph]
40. T. Sjöstrand, S. Mrenna, P.Z. Skands, A brief introduction to PYTHIA 8.1. Comput. Phys. Commun. **178**, 852 (2008). doi:10.1016/j.cpc.2008.01.036. arXiv:0710.3820 [hep-ph]
41. L. Lönnblad, Correcting the color dipole cascade model with fixed order matrix elements. JHEP **05**, 046 (2002). doi:10.1088/1126-6708/2002/05/046. arXiv:hep-ph/0112284
42. ATLAS Collaboration, ATLAS Pythia 8 tunes to 7 TeV data, ATL-PHYS-PUB-2014-021 (2014). https://cdsweb.cern.ch/record/1966419
43. R.D. Ball et al., Parton distributions with LHC data. Nucl. Phys. B **867**, 244 (2013). doi:10.1016/j.nuclphysb.2012.10.003. arXiv:1207.1303 [hep-ph]
44. R. Frederix, S. Frixione, Merging meets matching in MC@NLO. JHEP **12**, 061 (2012). doi:10.1007/JHEP12(2012)061. arXiv:1209.6215 [hep-ph]
45. R. Frederix, S. Frixione, A. Papaefstathiou, S. Prestel, P. Torrielli, A study of multi-jet production in association with an electroweak vector boson. JHEP **02**, 131 (2016). doi:10.1007/JHEP02(2016)131. arXiv:1511.00847 [hep-ph]
46. M.L. Mangano, M. Moretti, F. Piccinini, R. Pittau, A.D. Polosa, ALPGEN, a generator for hard multiparton processes in hadronic collisions. JHEP **07**, 001 (2003). doi:10.1088/1126-6708/2003/07/001. arXiv:hep-ph/0206293
47. T. Sjöstrand, S. Mrenna, P.Z. Skands, PYTHIA 6.4 physics and manual. JHEP **05**, 026 (2006). doi:10.1088/1126-6708/2006/05/026. arXiv:hep-ph/0603175
48. P.Z. Skands, Tuning Monte Carlo generators: the Perugia tunes. Phys. Rev. D **82**, 074018 (2010). doi:10.1103/PhysRevD.82.074018. arXiv:1005.3457 [hep-ph]
49. J. Pumplin et al., New generation of parton distributions with uncertainties from global QCD analysis. JHEP **07**, 012 (2002). doi:10.1088/1126-6708/2002/07/012. arXiv:hep-ph/0201195
50. H.-L. Lai et al., New parton distributions for collider physics. Phys. Rev. D **82**, 074024 (2010). doi:10.1103/PhysRevD.82.074024. arXiv:1007.2241 [hep-ph]
51. P. Nason, A new method for combining NLO QCD with shower Monte Carlo algorithms. JHEP **11**, 040 (2004). doi:10.1088/1126-6708/2004/11/040. arXiv:hep-ph/0409146
52. S. Frixione, P. Nason, C. Oleari, Matching NLO QCD computations with Parton shower simulations: the POWHEG method. JHEP **11**, 070 (2007). doi:10.1088/1126-6708/2007/11/070. arXiv:0709.2092 [hep-ph]
53. S. Alioli, P. Nason, C. Oleari, E. Re, A general framework for implementing NLO calculations in shower Monte Carlo programs: the POWHEG BOX. JHEP **06**, 043 (2010). doi:10.1007/JHEP06(2010)043. arXiv:1002.2581 [hep-ph]
54. M. Bahr et al., Herwig++ physics and manual. Eur. Phys. J. C **58**, 639 (2008). doi:10.1140/epjc/s10052-008-0798-9. arXiv:0803.0883 [hep-ph]
55. S. Gieseke, C. Rohr, A. Siodmok, Colour reconnections in Herwig++. Eur. Phys. J. C **72**, 2225 (2012). doi:10.1140/epjc/s10052-012-2225-5. arXiv:1206.0041 [hep-ph]
56. ATLAS Collaboration, Multi-boson simulation for 13 TeV ATLAS analyses, ATL-PHYS-PUB-2016-002 (2015). https://cdsweb.cern.ch/record/2119986
57. ATLAS Collaboration, Summary of ATLAS Pythia 8 tunes, ATLAS-PHYS-PUB-2012-003 (2012). https://cdsweb.cern.ch/record/1474107
58. A.D. Martin, W.J. Stirling, R.S. Thorne, G. Watt, Parton distributions for the LHC. Eur. Phys. J. C **63**, 189 (2009). doi:10.1140/epjc/s10052-009-1072-5. arXiv:0901.0002 [hep-ph]
59. C.F. Berger et al., Next-to-leading order QCD predictions for Z, γ^* + 3-Jet distributions at the Tevatron. Phys. Rev. D **82**, 074002 (2010). doi:10.1103/PhysRevD.82.074002. arXiv:1004.1659 [hep-ph]
60. H. Ita et al., Precise predictions for Z + 4 jets at Hadron colliders. Phys. Rev. D **85**, 031501 (2012). doi:10.1103/PhysRevD.85.031501. arXiv:1108.2229 [hep-ph]
61. S. Dulat et al., New parton distribution functions from a global analysis of quantum chromodynamics. Phys. Rev. D **93**, 033006 (2016). doi:10.1103/PhysRevD.93.033006. arXiv:1506.07443 [hep-ph]

62. R. Boughezal, C. Focke, X. Liu, F. Petriello, W-boson production in association with a jet at next-to-next-to-leading order in perturbative QCD. Phys. Rev. Lett. **115**, 062002 (2015). doi:10.1103/PhysRevLett.115.062002. arXiv:1504.02131 [hep-ph]
63. ATLAS Collaboration, Electron efficiency measurements with the ATLAS detector using the 2015 LHC proton-proton collision data, ATLAS-CONF-2016-024 (2016). https://cdsweb.cern.ch/record/2157687
64. ATLAS Collaboration, Electron identification measurements in ATLAS using $\sqrt{s}$ = 13 TeV data with 50 ns bunch spacing, ATL-PHYS-PUB-2015-041 (2015). https://cdsweb.cern.ch/record/2048202
65. ATLAS Collaboration, Muon reconstruction performance of the ATLAS detector in proton–proton collision data at $\sqrt{s}$ = 13 TeV. Eur. Phys. J. C **76**, 292 (2016). doi:10.1140/epjc/s10052-016-4120-y. arXiv:1603.05598 [hep-ex]
66. ATLAS Collaboration, Measurements of fiducial cross-sections for $t\bar{t}$ production with one or two additional b-jets in pp collisions at $\sqrt{s}$ = 8 TeV using the ATLAS detector. Eur. Phys. J. C **76**, 11 (2016). doi:10.1140/epjc/s10052-015-3852-4. arXiv:1508.06868 [hep-ex]
67. ATLAS Collaboration, Measurements of fiducial and differential cross sections for Higgs boson production in the diphoton decay channel at $\sqrt{s} = 8$ TeV with ATLAS. JHEP **09**, 112 (2014). doi:10.1007/JHEP09(2014)112. arXiv:1407.4222 [hep-ex]
68. M. Cacciari, G.P. Salam, G. Soyez, The anti-k_t jet clustering algorithm. JHEP **04**, 063 (2008). doi:10.1088/1126-6708/2008/04/063. arXiv:0802.1189 [hep-ph]
69. ATLAS Collaboration, Topological cell clustering in the ATLAS calorimeters and its performance in LHC Run 1 (2016). arXiv:1603.02934 [hep-ex]
70. ATLAS Collaboration, Jet Calibration and Systematic Uncertainties for Jets Reconstructed in the ATLAS Detector at $\sqrt{s}$ = 13 TeV, ATL-PHYS-PUB-2015-015 (2015). https://cdsweb.cern.ch/record/2028594
71. ATLAS Collaboration, Tagging and suppression of pileup jets with the ATLAS detector, ATLAS-CONF-2014-018 (2014). https://cds.cern.ch/record/1700870
72. ATLAS Collaboration, Performance of pile-up mitigation techniques for jets in pp collisions at $\sqrt{s}$ = 8 TeV using the ATLAS detector. Eur. Phys. J. C **76**, 581 (2016). doi:10.1140/epjc/s10052-016-4395-z. arXiv:1510.03823 [hep-ex]
73. ATLAS Collaboration, Improved luminosity determination in pp collisions at $\sqrt{s}$ = 7 TeV using the ATLAS detector at the LHC. Eur. Phys. J. C **73**, 2518 (2013). doi:10.1140/epjc/s10052-013-2518-3. arXiv:1302.4393 [hep-ex]
74. ATLAS Collaboration, Luminosity determination in pp collisions at $\sqrt{s}$ = 8 TeV using the ATLAS detector at the LHC, Eur. Phys. J. C **76**, 653 (2016). doi:10.1140/epjc/s10052-016-4466-1. arXiv:1608.03953 [hep-ex]
75. ATLAS Collaboration, Measurement of jets produced in top quark events using the di-lepton final state with 2 b-tagged jets in pp collisions at $\sqrt{s}$ = 13 TeV with the ATLAS detector, ATLAS-CONF-2015-065 (2015). https://cds.cern.ch/record/2114832
76. ATLAS Collaboration, Measurement of the $W^{\pm}Z$ boson pair-production cross section in pp collisions at $\sqrt{s}$ = 13 TeV with the ATLAS detector. Phys. Lett. B **762**, 1 (2016). doi:10.1016/j.physletb.2016.08.052. arXiv:1606.04017 [hep-ex]
77. G. D'Agostini, A multidimensional unfolding method based on Bayes' theorem. Nucl. Instrum. Meth. A **362**, 487 (1995). doi:10.1016/0168-9002(95)00274-X
78. The RooUnfold package and documentation are available from. http://hepunx.rl.ac.uk/~adye/software/unfold/RooUnfold.html
79. A. Glazov, Averaging of DIS cross section data. AIP Conf. Proc. **792**, 237 (2005). doi:10.1063/1.2122026
80. F.D. Aaron et al., Measurement of the Inclusive ep Scattering Cross Section at Low Q^2 and x at HERA. Eur. Phys. J. C **63**, 625 (2009). doi:10.1140/epjc/s10052-009-1128-6. arXiv:0904.0929 [hep-ex]
81. ATLAS Collaboration, Measurements of the W production cross sections in association with jets with the ATLAS detector. Eur. Phys. J. C **75**, 82 (2015). doi:10.1140/epjc/s10052-015-3262-7. arXiv:1409.8639 [hep-ex]
82. ATLAS Collaboration, ATLAS Computing Acknowledgements 2016–2017, ATL-GEN-PUB-2016-002. https://cdsweb.cern.ch/record/2202407

ATLAS Collaboration

M. Aaboud[137d], G. Aad[88], B. Abbott[115], J. Abdallah[8], O. Abdinov[12], B. Abeloos[119], R. Aben[109], O. S. AbouZeid[139], N. L. Abraham[151], H. Abramowicz[155], H. Abreu[154], R. Abreu[118], Y. Abulaiti[148a,148b], B. S. Acharya[167a,167b,a], S. Adachi[157], L. Adamczyk[41a], D. L. Adams[27], J. Adelman[110], S. Adomeit[102], T. Adye[133], A. A. Affolder[77], T. Agatonovic-Jovin[14], J. A. Aguilar-Saavedra[128a,128f], S. P. Ahlen[24], F. Ahmadov[68,b], G. Aielli[135a,135b], H. Akerstedt[148a,148b], T. P. A. Åkesson[84], A. V. Akimov[98], G. L. Alberghi[22a,22b], J. Albert[172], S. Albrand[58], M. J. Alconada Verzini[74], M. Aleksa[32], I. N. Aleksandrov[68], C. Alexa[28b], G. Alexander[155], T. Alexopoulos[10], M. Alhroob[115], B. Ali[130], M. Aliev[76a,76b], G. Alimonti[94a], J. Alison[33], S. P. Alkire[38], B. M. M. Allbrooke[151], B. W. Allen[118], P. P. Allport[19], A. Aloisio[106a,106b], A. Alonso[39], F. Alonso[74], C. Alpigiani[140], A. A. Alshehri[56], M. Alstaty[88], B. Alvarez Gonzalez[32], D. Álvarez Piqueras[170], M. G. Alviggi[106a,106b], B. T. Amadio[16], Y. Amaral Coutinho[26a], C. Amelung[25], D. Amidei[92], S. P. Amor Dos Santos[128a,128c], A. Amorim[128a,128b], S. Amoroso[32], G. Amundsen[25], C. Anastopoulos[141], L. S. Ancu[52], N. Andari[19], T. Andeen[11], C. F. Anders[60b], G. Anders[32], J. K. Anders[77], K. J. Anderson[33], A. Andreazza[94a,94b], V. Andrei[60a], S. Angelidakis[9], I. Angelozzi[109], A. Angerami[38], F. Anghinolfi[32], A. V. Anisenkov[111,c], N. Anjos[13], A. Annovi[126a,126b], C. Antel[60a], M. Antonelli[50], A. Antonov[100,*], D. J. Antrim[166], F. Anulli[134a], M. Aoki[69], L. Aperio Bella[19], G. Arabidze[93], Y. Arai[69], J. P. Araque[128a], A. T. H. Arce[48], F. A. Arduh[74], J-F. Arguin[97], S. Argyropoulos[66], M. Arik[20a], A. J. Armbruster[145], L. J. Armitage[79], O. Arnaez[32], H. Arnold[51], M. Arratia[30], O. Arslan[23], A. Artamonov[99], G. Artoni[122], S. Artz[86], S. Asai[157], N. Asbah[45], A. Ashkenazi[155], B. Åsman[148a,148b], L. Asquith[151], K. Assamagan[27], R. Astalos[146a], M. Atkinson[169], N. B. Atlay[143], K. Augsten[130], G. Avolio[32], B. Axen[16], M. K. Ayoub[119], G. Azuelos[97,d], M. A. Baak[32], A. E. Baas[60a], M. J. Baca[19], H. Bachacou[138], K. Bachas[76a,76b], M. Backes[122], M. Backhaus[32], P. Bagiacchi[134a,134b], P. Bagnaia[134a,134b], Y. Bai[35a], J. T. Baines[133], M. Bajic[39], O. K. Baker[179], E. M. Baldin[111,c], P. Balek[175], T. Balestri[150], F. Balli[138], W. K. Balunas[124], E. Banas[42], Sw. Banerjee[176,e], A. A. E. Bannoura[178], L. Barak[32], E. L. Barberio[91], D. Barberis[53a,53b], M. Barbero[88], T. Barillari[103], M-S Barisits[32], T. Barklow[145], N. Barlow[30], S. L. Barnes[87], B. M. Barnett[133], R. M. Barnett[16], Z. Barnovska-Blenessy[36a], A. Baroncelli[136a], G. Barone[25], A. J. Barr[122], L. Barranco Navarro[170], F. Barreiro[85], J. Barreiro Guimarães da Costa[35a], R. Bartoldus[145], A. E. Barton[75], P. Bartos[146a], A. Basalaev[125], A. Bassalat[119,f], R. L. Bates[56], S. J. Batista[161], J. R. Batley[30], M. Battaglia[139], M. Bauce[134a,134b], F. Bauer[138], H. S. Bawa[145,g], J. B. Beacham[113], M. D. Beattie[75], T. Beau[83], P. H. Beauchemin[165], P. Bechtle[23], H. P. Beck[18,h], K. Becker[122], M. Becker[86], M. Beckingham[173], C. Becot[112], A. J. Beddall[20d], A. Beddall[20b], V. A. Bednyakov[68], M. Bedognetti[109], C. P. Bee[150], L. J. Beemster[109], T. A. Beermann[32], M. Begel[27], J. K. Behr[45], A. S. Bell[81], G. Bella[155], L. Bellagamba[22a], A. Bellerive[31], M. Bellomo[89], K. Belotskiy[100], O. Beltramello[32], N. L. Belyaev[100], O. Benary[155,*], D. Benchekroun[137a], M. Bender[102], K. Bendtz[148a,148b], N. Benekos[10], Y. Benhammou[155], E. Benhar Noccioli[179], J. Benitez[66], D. P. Benjamin[48], J. R. Bensinger[25], S. Bentvelsen[109], L. Beresford[122], M. Beretta[50], D. Berge[109], E. Bergeaas Kuutmann[168], N. Berger[5], J. Beringer[16], S. Berlendis[58], N. R. Bernard[89], C. Bernius[112], F. U. Bernlochner[23], T. Berry[80], P. Berta[131], C. Bertella[86], G. Bertoli[148a,148b], F. Bertolucci[126a,126b], I. A. Bertram[75], C. Bertsche[45], D. Bertsche[115], G. J. Besjes[39], O. Bessidskaia Bylund[148a,148b], M. Bessner[45], N. Besson[138], C. Betancourt[51], A. Bethani[58], S. Bethke[103], A. J. Bevan[79], R. M. Bianchi[127], M. Bianco[32], O. Biebel[102], D. Biedermann[17], R. Bielski[87], N. V. Biesuz[126a,126b], M. Biglietti[136a], J. Bilbao De Mendizabal[52], T. R. V. Billoud[97], H. Bilokon[50], M. Bindi[57], A. Bingul[20b], C. Bini[134a,134b], S. Biondi[22a,22b], T. Bisanz[57], D. M. Bjergaard[48], C. W. Black[152], J. E. Black[145], K. M. Black[24], D. Blackburn[140], R. E. Blair[6], T. Blazek[146a], I. Bloch[45], C. Blocker[25], A. Blue[56], W. Blum[86,*], U. Blumenschein[57], S. Blunier[34a], G. J. Bobbink[109], V. S. Bobrovnikov[111,c], S. S. Bocchetta[84], A. Bocci[48], C. Bock[102], M. Boehler[51], D. Boerner[178], J. A. Bogaerts[32], D. Bogavac[14], A. G. Bogdanchikov[111], C. Bohm[148a], V. Boisvert[80], P. Bokan[14], T. Bold[41a], A. S. Boldyrev[101], M. Bomben[83], M. Bona[79], M. Boonekamp[138], A. Borisov[132], G. Borissov[75], J. Bortfeldt[32], D. Bortoletto[122], V. Bortolotto[62a,62b,62c], K. Bos[109], D. Boscherini[22a], M. Bosman[13], J. D. Bossio Sola[29], J. Boudreau[127], J. Bouffard[2], E. V. Bouhova-Thacker[75], D. Boumediene[37], C. Bourdarios[119], S. K. Boutle[56], A. Boveia[32], J. Boyd[32], I. R. Boyko[68], J. Bracinik[19], A. Brandt[8], G. Brandt[57], O. Brandt[60a], U. Bratzler[158], B. Brau[89], J. E. Brau[118], W. D. Breaden Madden[56], K. Brendlinger[124], A. J. Brennan[91], L. Brenner[109], R. Brenner[168], S. Bressler[175], T. M. Bristow[49], D. Britton[56], D. Britzger[45], F. M. Brochu[30], I. Brock[23], R. Brock[93], G. Brooijmans[38], T. Brooks[80], W. K. Brooks[34b], J. Brosamer[16], E. Brost[110], J. H Broughton[19], P. A. Bruckman de Renstrom[42], D. Bruncko[146b], R. Bruneliere[51], A. Bruni[22a], G. Bruni[22a], L. S. Bruni[109], BH Brunt[30], M. Bruschi[22a], N. Bruscino[23], P. Bryant[33], L. Bryngemark[84], T. Buanes[15], Q. Buat[144], P. Buchholz[143], A. G. Buckley[56], I. A. Budagov[68], F. Buehrer[51], M. K. Bugge[121], O. Bulekov[100], D. Bullock[8], H. Burckhart[32], S. Burdin[77], C. D. Burgard[51], A. M. Burger[5], B. Burghgrave[110], K. Burka[42], S. Burke[133], I. Burmeister[46], J. T. P. Burr[122], E. Busato[37], D. Büscher[51], V. Büscher[86], P. Bussey[56], J. M. Butler[24], C. M. Buttar[56], J. M. Butterworth[81], P. Butti[109], W. Buttinger[27], A. Buzatu[56], A. R. Buzykaev[111,c], S. Cabrera Urbán[170], D. Caforio[130],

V. M. Cairo[40a,40b], O. Cakir[4a], N. Calace[52], P. Calafiura[16], A. Calandri[88], G. Calderini[83], P. Calfayan[64], G. Callea[40a,40b], L. P. Caloba[26a], S. Calvente Lopez[85], D. Calvet[37], S. Calvet[37], T. P. Calvet[88], R. Camacho Toro[33], S. Camarda[32], P. Camarri[135a,135b], D. Cameron[121], R. Caminal Armadans[169], C. Camincher[58], S. Campana[32], M. Campanelli[81], A. Camplani[94a,94b], A. Campoverde[143], V. Canale[106a,106b], A. Canepa[163a], M. Cano Bret[36c], J. Cantero[116], T. Cao[43], M. D. M. Capeans Garrido[32], I. Caprini[28b], M. Caprini[28b], M. Capua[40a,40b], R. M. Carbone[38], R. Cardarelli[135a], F. Cardillo[51], I. Carli[131], T. Carli[32], G. Carlino[106a], L. Carminati[94a,94b], R. M. D. Carney[148a,148b], S. Caron[108], E. Carquin[34b], G. D. Carrillo-Montoya[32], J. R. Carter[30], J. Carvalho[128a,128c], D. Casadei[19], M. P. Casado[13,i], M. Casolino[13], D. W. Casper[166], E. Castaneda-Miranda[147a], R. Castelijn[109], A. Castelli[109], V. Castillo Gimenez[170], N. F. Castro[128a,j], A. Catinaccio[32], J. R. Catmore[121], A. Cattai[32], J. Caudron[23], V. Cavaliere[169], E. Cavallaro[13], D. Cavalli[94a], M. Cavalli-Sforza[13], V. Cavasinni[126a,126b], F. Ceradini[136a,136b], L. Cerda Alberich[170], A. S. Cerqueira[26b], A. Cerri[151], L. Cerrito[135a,135b], F. Cerutti[16], A. Cervelli[18], S. A. Cetin[20c], A. Chafaq[137a], D. Chakraborty[110], S. K. Chan[59], Y. L. Chan[62a], P. Chang[169], J. D. Chapman[30], D. G. Charlton[19], A. Chatterjee[52], C. C. Chau[161], C. A. Chavez Barajas[151], S. Che[113], S. Cheatham[167a,167c], A. Chegwidden[93], S. Chekanov[6], S. V. Chekulaev[163a], G. A. Chelkov[68,k], M. A. Chelstowska[92], C. Chen[67], H. Chen[27], K. Chen[150], S. Chen[35b], S. Chen[157], X. Chen[35c,l], Y. Chen[70], H. C. Cheng[92], H. J. Cheng[35a], Y. Cheng[33], A. Cheplakov[68], E. Cheremushkina[132], R. Cherkaoui El Moursli[137e], V. Chernyatin[27,*], E. Cheu[7], L. Chevalier[138], V. Chiarella[50], G. Chiarelli[126a,126b], G. Chiodini[76a], A. S. Chisholm[32], A. Chitan[28b], M. V. Chizhov[68], K. Choi[64], A. R. Chomont[37], S. Chouridou[9], B. K. B. Chow[102], V. Christodoulou[81], D. Chromek-Burckhart[32], J. Chudoba[129], A. J. Chuinard[90], J. J. Chwastowski[42], L. Chytka[117], G. Ciapetti[134a,134b], A. K. Ciftci[4a], D. Cinca[46], V. Cindro[78], I. A. Cioara[23], C. Ciocca[22a,22b], A. Ciocio[16], F. Cirotto[106a,106b], Z. H. Citron[175], M. Citterio[94a], M. Ciubancan[28b], A. Clark[52], B. L. Clark[59], M. R. Clark[38], P. J. Clark[49], R. N. Clarke[16], C. Clement[148a,148b], Y. Coadou[88], M. Cobal[167a,167c], A. Coccaro[52], J. Cochran[67], L. Colasurdo[108], B. Cole[38], A. P. Colijn[109], J. Collot[58], T. Colombo[166], G. Compostella[103], P. Conde Muiño[128a,128b], E. Coniavitis[51], S. H. Connell[147b], I. A. Connelly[80], V. Consorti[51], S. Constantinescu[28b], G. Conti[32], F. Conventi[106a,m], M. Cooke[16], B. D. Cooper[81], A. M. Cooper-Sarkar[122], F. Cormier[171], K. J. R. Cormier[161], T. Cornelissen[178], M. Corradi[134a,134b], F. Corriveau[90,n], A. Cortes-Gonzalez[32], G. Cortiana[103], G. Costa[94a], M. J. Costa[170], D. Costanzo[141], G. Cottin[30], G. Cowan[80], B. E. Cox[87], K. Cranmer[112], S. J. Crawley[56], G. Cree[31], S. Crépé-Renaudin[58], F. Crescioli[83], W. A. Cribbs[148a,148b], M. Crispin Ortuzar[122], M. Cristinziani[23], V. Croft[108], G. Crosetti[40a,40b], A. Cueto[85], T. Cuhadar Donszelmann[141], J. Cummings[179], M. Curatolo[50], J. Cúth[86], H. Czirr[143], P. Czodrowski[3], G. D'amen[22a,22b], S. D'Auria[56], M. D'Onofrio[77], M. J. Da Cunha Sargedas De Sousa[128a,128b], C. Da Via[87], W. Dabrowski[41a], T. Dado[146a], T. Dai[92], O. Dale[15], F. Dallaire[97], C. Dallapiccola[89], M. Dam[39], J. R. Dandoy[33], N. P. Dang[51], A. C. Daniells[19], N. S. Dann[87], M. Danninger[171], M. Dano Hoffmann[138], V. Dao[51], G. Darbo[53a], S. Darmora[8], J. Dassoulas[3], A. Dattagupta[118], W. Davey[23], C. David[172], T. Davidek[131], M. Davies[155], P. Davison[81], E. Dawe[91], I. Dawson[141], K. De[8], R. de Asmundis[106a], A. De Benedetti[115], S. De Castro[22a,22b], S. De Cecco[83], N. De Groot[108], P. de Jong[109], H. De la Torre[93], F. De Lorenzi[67], A. De Maria[57], D. De Pedis[134a], A. De Salvo[134a], U. De Sanctis[151], A. De Santo[151], J. B. De Vivie De Regie[119], W. J. Dearnaley[75], R. Debbe[27], C. Debenedetti[139], D. V. Dedovich[68], N. Dehghanian[3], I. Deigaard[109], M. Del Gaudio[40a,40b], J. Del Peso[85], T. Del Prete[126a,126b], D. Delgove[119], F. Deliot[138], C. M. Delitzsch[52], A. Dell'Acqua[32], L. Dell'Asta[24], M. Dell'Orso[126a,126b], M. Della Pietra[106a,m], D. della Volpe[52], M. Delmastro[5], P. A. Delsart[58], D. A. DeMarco[161], S. Demers[179], M. Demichev[68], A. Demilly[83], S. P. Denisov[132], D. Denysiuk[138], D. Derendarz[42], J. E. Derkaoui[137d], F. Derue[83], P. Dervan[77], K. Desch[23], C. Deterre[45], K. Dette[46], P. O. Deviveiros[32], A. Dewhurst[133], S. Dhaliwal[25], A. Di Ciaccio[135a,135b], L. Di Ciaccio[5], W. K. Di Clemente[124], C. Di Donato[106a,106b], A. Di Girolamo[32], B. Di Girolamo[32], B. Di Micco[136a,136b], R. Di Nardo[32], K. F. Di Petrillo[59], A. Di Simone[51], R. Di Sipio[161], D. Di Valentino[31], C. Diaconu[88], M. Diamond[161], F. A. Dias[49], M. A. Diaz[34a], E. B. Diehl[92], J. Dietrich[17], S. Díez Cornell[45], A. Dimitrievska[14], J. Dingfelder[23], P. Dita[28b], S. Dita[28b], F. Dittus[32], F. Djama[88], T. Djobava[54b], J. I. Djuvsland[60a], M. A. B. do Vale[26c], D. Dobos[32], M. Dobre[28b], C. Doglioni[84], J. Dolejsi[131], Z. Dolezal[131], M. Donadelli[26d], S. Donati[126a,126b], P. Dondero[123a,123b], J. Donini[37], J. Dopke[133], A. Doria[106a], M. T. Dova[74], A. T. Doyle[56], E. Drechsler[57], M. Dris[10], Y. Du[36b], J. Duarte-Campderros[155], E. Duchovni[175], G. Duckeck[102], O. A. Ducu[97,o], D. Duda[109], A. Dudarev[32], A. Chr. Dudder[86], E. M. Duffield[16], L. Duflot[119], M. Dührssen[32], M. Dumancic[175], A. K. Duncan[56], M. Dunford[60a], H. Duran Yildiz[4a], M. Düren[55], A. Durglishvili[54b], D. Duschinger[47], B. Dutta[45], M. Dyndal[45], C. Eckardt[45], K. M. Ecker[103], R. C. Edgar[92], N. C. Edwards[49], T. Eifert[32], G. Eigen[15], K. Einsweiler[16], T. Ekelof[168], M. El Kacimi[137c], V. Ellajosyula[88], M. Ellert[168], S. Elles[5], F. Ellinghaus[178], A. A. Elliot[172], N. Ellis[32], J. Elmsheuser[27], M. Elsing[32], D. Emeliyanov[133], Y. Enari[157], O. C. Endner[86], J. S. Ennis[173], J. Erdmann[46], A. Ereditato[18], G. Ernis[178], J. Ernst[2], M. Ernst[27], S. Errede[169], E. Ertel[86], M. Escalier[119], H. Esch[46], C. Escobar[127], B. Esposito[50], A. I. Etienvre[138], E. Etzion[155], H. Evans[64], A. Ezhilov[125], F. Fabbri[22a,22b], L. Fabbri[22a,22b], G. Facini[33], R. M. Fakhrutdinov[132], S. Falciano[134a], R. J. Falla[81], J. Faltova[32], Y. Fang[35a], M. Fanti[94a,94b], A. Farbin[8],

A. Farilla[136a], C. Farina[127], E. M. Farina[123a,123b], T. Farooque[13], S. Farrell[16], S. M. Farrington[173], P. Farthouat[32], F. Fassi[137e], P. Fassnacht[32], D. Fassouliotis[9], M. Faucci Giannelli[80], A. Favareto[53a,53b], W. J. Fawcett[122], L. Fayard[119], O. L. Fedin[125,p], W. Fedorko[171], S. Feigl[121], L. Feligioni[88], C. Feng[36b], E. J. Feng[32], H. Feng[92], A. B. Fenyuk[132], L. Feremenga[8], P. Fernandez Martinez[170], S. Fernandez Perez[13], J. Ferrando[45], A. Ferrari[168], P. Ferrari[109], R. Ferrari[123a], D. E. Ferreira de Lima[60b], A. Ferrer[170], D. Ferrere[52], C. Ferretti[92], F. Fiedler[86], A. Filipčič[78], M. Filipuzzi[45], F. Filthaut[108], M. Fincke-Keeler[172], K. D. Finelli[152], M. C. N. Fiolhais[128a,128c], L. Fiorini[170], A. Fischer[2], C. Fischer[13], J. Fischer[178], W. C. Fisher[93], N. Flaschel[45], I. Fleck[143], P. Fleischmann[92], G. T. Fletcher[141], R. R. M. Fletcher[124], T. Flick[178], B. M. Flierl[102], L. R. Flores Castillo[62a], M. J. Flowerdew[103], G. T. Forcolin[87], A. Formica[138], A. Forti[87], A. G. Foster[19], D. Fournier[119], H. Fox[75], S. Fracchia[13], P. Francavilla[83], M. Franchini[22a,22b], D. Francis[32], L. Franconi[121], M. Franklin[59], M. Frate[166], M. Fraternali[123a,123b], D. Freeborn[81], S. M. Fressard-Batraneanu[32], F. Friedrich[47], D. Froidevaux[32], J. A. Frost[122], C. Fukunaga[158], E. Fullana Torregrosa[86], T. Fusayasu[104], J. Fuster[170], C. Gabaldon[58], O. Gabizon[154], A. Gabrielli[22a,22b], A. Gabrielli[16], G. P. Gach[41a], S. Gadatsch[32], G. Gagliardi[53a,53b], L. G. Gagnon[97], P. Gagnon[64], C. Galea[108], B. Galhardo[128a,128c], E. J. Gallas[122], B. J. Gallop[133], P. Gallus[130], G. Galster[39], K. K. Gan[113], S. Ganguly[37], J. Gao[36a], Y. Gao[49], Y. S. Gao[145,g], F. M. Garay Walls[49], C. García[170], J. E. García Navarro[170], M. Garcia-Sciveres[16], R. W. Gardner[33], N. Garelli[145], V. Garonne[121], A. Gascon Bravo[45], K. Gasnikova[45], C. Gatti[50], A. Gaudiello[53a,53b], G. Gaudio[123a], L. Gauthier[97], I. L. Gavrilenko[98], C. Gay[171], G. Gaycken[23], E. N. Gazis[10], Z. Gecse[171], C. N. P. Gee[133], Ch. Geich-Gimbel[23], M. Geisen[86], M. P. Geisler[60a], K. Gellerstedt[148a,148b], C. Gemme[53a], M. H. Genest[58], C. Geng[36a,q], S. Gentile[134a,134b], C. Gentsos[156], S. George[80], D. Gerbaudo[13], A. Gershon[155], S. Ghasemi[143], M. Ghneimat[23], B. Giacobbe[22a], S. Giagu[134a,134b], P. Giannetti[126a,126b], S. M. Gibson[80], M. Gignac[171], M. Gilchriese[16], T. P. S. Gillam[30], D. Gillberg[31], G. Gilles[178], D. M. Gingrich[3,d], N. Giokaris[9,*], M. P. Giordani[167a,167c], F. M. Giorgi[22a], P. F. Giraud[138], P. Giromini[59], D. Giugni[94a], F. Giuli[122], C. Giuliani[103], M. Giulini[60b], B. K. Gjelsten[121], S. Gkaitatzis[156], I. Gkialas[9], E. L. Gkougkousis[119], L. K. Gladilin[101], C. Glasman[85], J. Glatzer[13], P. C. F. Glaysher[49], A. Glazov[45], M. Goblirsch-Kolb[25], J. Godlewski[42], S. Goldfarb[91], T. Golling[52], D. Golubkov[132], A. Gomes[128a,128b,128d], R. Gonçalo[128a], J. Goncalves Pinto Firmino Da Costa[138], G. Gonella[51], L. Gonella[19], A. Gongadze[68], S. González de la Hoz[170], S. Gonzalez-Sevilla[52], L. Goossens[32], P. A. Gorbounov[99], H. A. Gordon[27], I. Gorelov[107], B. Gorini[32], E. Gorini[76a,76b], A. Gorišek[78], E. Gornicki[42], A. T. Goshaw[48], C. Gössling[46], M. I. Gostkin[68], C. R. Goudet[119], D. Goujdami[137c], A. G. Goussiou[140], N. Govender[147b,r], E. Gozani[154], L. Graber[57], I. Grabowska-Bold[41a], P. O. J. Gradin[58], P. Grafström[22a,22b], J. Gramling[52], E. Gramstad[121], S. Grancagnolo[17], V. Gratchev[125], P. M. Gravila[28e], H. M. Gray[32], E. Graziani[136a], Z. D. Greenwood[82,s], C. Grefe[23], K. Gregersen[81], I. M. Gregor[45], P. Grenier[145], K. Grevtsov[5], J. Griffiths[8], A. A. Grillo[139], K. Grimm[75], S. Grinstein[13,t], Ph. Gris[37], J.-F. Grivaz[119], S. Groh[86], E. Gross[175], J. Grosse-Knetter[57], G. C. Grossi[82], Z. J. Grout[81], L. Guan[92], W. Guan[176], J. Guenther[65], F. Guescini[52], D. Guest[166], O. Gueta[155], B. Gui[113], E. Guido[53a,53b], T. Guillemin[5], S. Guindon[2], U. Gul[56], C. Gumpert[32], J. Guo[36c], Y. Guo[36a,q], R. Gupta[43], S. Gupta[122], G. Gustavino[134a,134b], P. Gutierrez[115], N. G. Gutierrez Ortiz[81], C. Gutschow[81], C. Guyot[138], C. Gwenlan[122], C. B. Gwilliam[77], A. Haas[112], C. Haber[16], H. K. Hadavand[8], A. Hadef[88], S. Hageböck[23], M. Hagihara[164], Z. Hajduk[42], H. Hakobyan[180,*], M. Haleem[45], J. Haley[116], G. Halladjian[93], G. D. Hallewell[88], K. Hamacher[178], P. Hamal[117], K. Hamano[172], A. Hamilton[147a], G. N. Hamity[141], P. G. Hamnett[45], L. Han[36a], K. Hanagaki[69,u], K. Hanawa[157], M. Hance[139], B. Haney[124], P. Hanke[60a], R. Hanna[138], J. B. Hansen[39], J. D. Hansen[39], M. C. Hansen[23], P. H. Hansen[39], K. Hara[164], A. S. Hard[176], T. Harenberg[178], F. Hariri[119], S. Harkusha[95], R. D. Harrington[49], P. F. Harrison[173], F. Hartjes[109], N. M. Hartmann[102], M. Hasegawa[70], Y. Hasegawa[142], A. Hasib[115], S. Hassani[138], S. Haug[18], R. Hauser[93], L. Hauswald[47], M. Havranek[129], C. M. Hawkes[19], R. J. Hawkings[32], D. Hayakawa[159], D. Hayden[93], C. P. Hays[122], J. M. Hays[79], H. S. Hayward[77], S. J. Haywood[133], S. J. Head[19], T. Heck[86], V. Hedberg[84], L. Heelan[8], S. Heim[124], T. Heim[16], B. Heinemann[16], J. J. Heinrich[102], L. Heinrich[112], C. Heinz[55], J. Hejbal[129], L. Helary[32], S. Hellman[148a,148b], C. Helsens[32], J. Henderson[122], R. C. W. Henderson[75], Y. Heng[176], S. Henkelmann[171], A. M. Henriques Correia[32], S. Henrot-Versille[119], G. H. Herbert[17], H. Herde[25], V. Herget[177], Y. Hernández Jiménez[147c], G. Herten[51], R. Hertenberger[102], L. Hervas[32], G. G. Hesketh[81], N. P. Hessey[109], J. W. Hetherly[43], E. Higón-Rodriguez[170], E. Hill[172], J. C. Hill[30], K. H. Hiller[45], S. J. Hillier[19], I. Hinchliffe[16], E. Hines[124], R. R. Hinman[16], M. Hirose[51], D. Hirschbuehl[178], X. Hoad[49], J. Hobbs[150], N. Hod[163a], M. C. Hodgkinson[141], P. Hodgson[141], A. Hoecker[32], M. R. Hoeferkamp[107], F. Hoenig[102], D. Hohn[23], T. R. Holmes[16], M. Homann[46], T. Honda[69], T. M. Hong[127], B. H. Hooberman[169], W. H. Hopkins[118], Y. Horii[105], A. J. Horton[144], J-Y. Hostachy[58], S. Hou[153], A. Hoummada[137a], J. Howarth[45], J. Hoya[74], M. Hrabovsky[117], I. Hristova[17], J. Hrivnac[119], T. Hryn'ova[5], A. Hrynevich[96], P. J. Hsu[63], S.-C. Hsu[140], Q. Hu[36a], S. Hu[36c], Y. Huang[45], Z. Hubacek[130], F. Hubaut[88], F. Huegging[23], T. B. Huffman[122], E. W. Hughes[38], G. Hughes[75], M. Huhtinen[32], P. Huo[150], N. Huseynov[68,b], J. Huston[93], J. Huth[59], G. Iacobucci[52], G. Iakovidis[27], I. Ibragimov[143], L. Iconomidou-Fayard[119], E. Ideal[179], P. Iengo[32], O. Igonkina[109,v],

T. Iizawa[174], Y. Ikegami[69], M. Ikeno[69], Y. Ilchenko[11,w], D. Iliadis[156], N. Ilic[145], G. Introzzi[123a,123b], P. Ioannou[9,*], M. Iodice[136a], K. Iordanidou[38], V. Ippolito[59], N. Ishijima[120], M. Ishino[157], M. Ishitsuka[159], R. Ishmukhametov[113], C. Issever[122], S. Istin[20a], F. Ito[164], J. M. Iturbe Ponce[87], R. Iuppa[162a,162b], W. Iwanski[65], H. Iwasaki[69], J. M. Izen[44], V. Izzo[106a], S. Jabbar[3], B. Jackson[124], P. Jackson[1], V. Jain[2], K. B. Jakobi[86], K. Jakobs[51], S. Jakobsen[32], T. Jakoubek[129], D. O. Jamin[116], D. K. Jana[82], R. Jansky[65], J. Janssen[23], M. Janus[57], P. A. Janus[41a], G. Jarlskog[84], N. Javadov[68,b], T. Javůrek[51], M. Javurkova[51], F. Jeanneau[138], L. Jeanty[16], J. Jejelava[54a,x], G.-Y. Jeng[152], D. Jennens[91], P. Jenni[51,y], C. Jeske[173], S. Jézéquel[5], H. Ji[176], J. Jia[150], H. Jiang[67], Y. Jiang[36a], Z. Jiang[145], S. Jiggins[81], J. Jimenez Pena[170], S. Jin[35a], A. Jinaru[28b], O. Jinnouchi[159], H. Jivan[147c], P. Johansson[141], K. A. Johns[7], W. J. Johnson[140], K. Jon-And[148a,148b], G. Jones[173], R. W. L. Jones[75], S. Jones[7], T. J. Jones[77], J. Jongmanns[60a], P. M. Jorge[128a,128b], J. Jovicevic[163a], X. Ju[176], A. Juste Rozas[13,t], M. K. Köhler[175], A. Kaczmarska[42], M. Kado[119], H. Kagan[113], M. Kagan[145], S. J. Kahn[88], T. Kaji[174], E. Kajomovitz[48], C. W. Kalderon[122], A. Kaluza[86], S. Kama[43], A. Kamenshchikov[132], N. Kanaya[157], S. Kaneti[30], L. Kanjir[78], V. A. Kantserov[100], J. Kanzaki[69], B. Kaplan[112], L. S. Kaplan[176], A. Kapliy[33], D. Kar[147c], K. Karakostas[10], A. Karamaoun[3], N. Karastathis[10], M. J. Kareem[57], E. Karentzos[10], M. Karnevskiy[86], S. N. Karpov[68], Z. M. Karpova[68], K. Karthik[112], V. Kartvelishvili[75], A. N. Karyukhin[132], K. Kasahara[164], L. Kashif[176], R. D. Kass[113], A. Kastanas[149], Y. Kataoka[157], C. Kato[157], A. Katre[52], J. Katzy[45], K. Kawade[105], K. Kawagoe[73], T. Kawamoto[157], G. Kawamura[57], V. F. Kazanin[111,c], R. Keeler[172], R. Kehoe[43], J. S. Keller[45], J. J. Kempster[80], H. Keoshkerian[161], O. Kepka[129], B. P. Kerševan[78], S. Kersten[178], R. A. Keyes[90], M. Khader[169], F. Khalil-zada[12], A. Khanov[116], A. G. Kharlamov[111,c], T. Kharlamova[111,c], T. J. Khoo[52], V. Khovanskiy[99], E. Khramov[68], J. Khubua[54b,z], S. Kido[70], C. R. Kilby[80], H. Y. Kim[8], S. H. Kim[164], Y. K. Kim[33], N. Kimura[156], O. M. Kind[17], B. T. King[77], M. King[170], J. Kirk[133], A. E. Kiryunin[103], T. Kishimoto[157], D. Kisielewska[41a], F. Kiss[51], K. Kiuchi[164], O. Kivernyk[138], E. Kladiva[146b], M. H. Klein[38], M. Klein[77], U. Klein[77], K. Kleinknecht[86], P. Klimek[110], A. Klimentov[27], R. Klingenberg[46], T. Klioutchnikova[32], E.-E. Kluge[60a], P. Kluit[109], S. Kluth[103], J. Knapik[42], E. Kneringer[65], E. B. F. G. Knoops[88], A. Knue[103], A. Kobayashi[157], D. Kobayashi[159], T. Kobayashi[157], M. Kobel[47], M. Kocian[145], P. Kodys[131], T. Koffas[31], E. Koffeman[109], N. M. Köhler[103], T. Koi[145], H. Kolanoski[17], M. Kolb[60b], I. Koletsou[5], A. A. Komar[98,*], Y. Komori[157], T. Kondo[69], N. Kondrashova[36c], K. Köneke[51], A. C. König[108], T. Kono[69,aa], R. Konoplich[112,ab], N. Konstantinidis[81], R. Kopeliansky[64], S. Koperny[41a], L. Köpke[86], A. K. Kopp[51], K. Korcyl[42], K. Kordas[156], A. Korn[81], A. A. Korol[111,c], I. Korolkov[13], E. V. Korolkova[141], O. Kortner[103], S. Kortner[103], T. Kosek[131], V. V. Kostyukhin[23], A. Kotwal[48], A. Koulouris[10], A. Kourkoumeli-Charalampidi[123a,123b], C. Kourkoumelis[9], V. Kouskoura[27], A. B. Kowalewska[42], R. Kowalewski[172], T. Z. Kowalski[41a], C. Kozakai[157], W. Kozanecki[138], A. S. Kozhin[132], V. A. Kramarenko[101], G. Kramberger[78], D. Krasnopevtsev[100], M. W. Krasny[83], A. Krasznahorkay[32], A. Kravchenko[27], M. Kretz[60c], J. Kretzschmar[77], K. Kreutzfeldt[55], P. Krieger[161], K. Krizka[33], K. Kroeninger[46], H. Kroha[103], J. Kroll[124], J. Kroseberg[23], J. Krstic[14], U. Kruchonak[68], H. Krüger[23], N. Krumnack[67], M. C. Kruse[48], M. Kruskal[24], T. Kubota[91], H. Kucuk[81], S. Kuday[4b], J. T. Kuechler[178], S. Kuehn[51], A. Kugel[60c], F. Kuger[177], T. Kuhl[45], V. Kukhtin[68], R. Kukla[138], Y. Kulchitsky[95], S. Kuleshov[34b], M. Kuna[134a,134b], T. Kunigo[71], A. Kupco[129], H. Kurashige[70], L. L. Kurchaninov[163a], Y. A. Kurochkin[95], M. G. Kurth[44], V. Kus[129], E. S. Kuwertz[172], M. Kuze[159], J. Kvita[117], T. Kwan[172], D. Kyriazopoulos[141], A. La Rosa[103], J. L. La Rosa Navarro[26d], L. La Rotonda[40a,40b], C. Lacasta[170], F. Lacava[134a,134b], J. Lacey[31], H. Lacker[17], D. Lacour[83], V. R. Lacuesta[170], E. Ladygin[68], R. Lafaye[5], B. Laforge[83], T. Lagouri[179], S. Lai[57], S. Lammers[64], W. Lampl[7], E. Lançon[138], U. Landgraf[51], M. P. J. Landon[79], M. C. Lanfermann[52], V. S. Lang[60a], J. C. Lange[13], A. J. Lankford[166], F. Lanni[27], K. Lantzsch[23], A. Lanza[123a], S. Laplace[83], C. Lapoire[32], J. F. Laporte[138], T. Lari[94a], F. Lasagni Manghi[22a,22b], M. Lassnig[32], P. Laurelli[50], W. Lavrijsen[16], A. T. Law[139], P. Laycock[77], T. Lazovich[59], M. Lazzaroni[94a,94b], B. Le[91], O. Le Dortz[83], E. Le Guirriec[88], E. P. Le Quilleuc[138], M. LeBlanc[172], T. LeCompte[6], F. Ledroit-Guillon[58], C. A. Lee[27], S. C. Lee[153], L. Lee[1], B. Lefebvre[90], G. Lefebvre[83], M. Lefebvre[172], F. Legger[102], C. Leggett[16], A. Lehan[77], G. Lehmann Miotto[32], X. Lei[7], W. A. Leight[31], A. G. Leister[179], M. A. L. Leite[26d], R. Leitner[131], D. Lellouch[175], B. Lemmer[57], K. J. C. Leney[81], T. Lenz[23], B. Lenzi[32], R. Leone[7], S. Leone[126a,126b], C. Leonidopoulos[49], S. Leontsinis[10], G. Lerner[151], C. Leroy[97], A. A. J. Lesage[138], C. G. Lester[30], M. Levchenko[125], J. Levêque[5], D. Levin[92], L. J. Levinson[175], M. Levy[19], D. Lewis[79], M. Leyton[44], B. Li[36a,q], C. Li[36a], H. Li[150], L. Li[48], L. Li[36c], Q. Li[35a], S. Li[48], X. Li[87], Y. Li[143], Z. Liang[35a], B. Liberti[135a], A. Liblong[161], P. Lichard[32], K. Lie[169], J. Liebal[23], W. Liebig[15], A. Limosani[152], S. C. Lin[153,ac], T. H. Lin[86], B. E. Lindquist[150], A. E. Lionti[52], E. Lipeles[124], A. Lipniacka[15], M. Lisovyi[60b], T. M. Liss[169], A. Lister[171], A. M. Litke[139], B. Liu[153,ad], D. Liu[153], H. Liu[92], H. Liu[27], J. Liu[36b], J. B. Liu[36a], K. Liu[88], L. Liu[169], M. Liu[36a], Y. L. Liu[36a], Y. Liu[36a], M. Livan[123a,123b], A. Lleres[58], J. Llorente Merino[35a], S. L. Lloyd[79], F. Lo Sterzo[153], E. M. Lobodzinska[45], P. Loch[7], F. K. Loebinger[87], K. M. Loew[25], A. Loginov[179,*], T. Lohse[17], K. Lohwasser[45], M. Lokajicek[129], B. A. Long[24], J. D. Long[169], R. E. Long[75], L. Longo[76a,76b], K. A. Looper[113], J. A. Lopez[34b], D. Lopez Mateos[59], B. Lopez Paredes[141], I. Lopez Paz[13], A. Lopez Solis[83], J. Lorenz[102], N. Lorenzo Martinez[64], M. Losada[21], P. J. Lösel[102], X. Lou[35a],

A. Lounis[119], J. Love[6], P. A. Love[75], H. Lu[62a], N. Lu[92], H. J. Lubatti[140], C. Luci[134a,134b], A. Lucotte[58], C. Luedtke[51], F. Luehring[64], W. Lukas[65], L. Luminari[134a], O. Lundberg[148a,148b], B. Lund-Jensen[149], P. M. Luzi[83], D. Lynn[27], R. Lysak[129], E. Lytken[84], V. Lyubushkin[68], H. Ma[27], L. L. Ma[36b], Y. Ma[36b], G. Maccarrone[50], A. Macchiolo[103], C. M. Macdonald[141], B. Maček[78], J. Machado Miguens[124,128b], D. Madaffari[88], R. Madar[37], H. J. Maddocks[168], W. F. Mader[47], A. Madsen[45], J. Maeda[70], S. Maeland[15], T. Maeno[27], A. Maevskiy[101], E. Magradze[57], J. Mahlstedt[109], C. Maiani[119], C. Maidantchik[26a], A. A. Maier[103], T. Maier[102], A. Maio[128a,128b,128d], S. Majewski[118], Y. Makida[69], N. Makovec[119], B. Malaescu[83], Pa. Malecki[42], V. P. Maleev[125], F. Malek[58], U. Mallik[66], D. Malon[6], C. Malone[145], C. Malone[30], S. Maltezos[10], S. Malyukov[32], J. Mamuzic[170], G. Mancini[50], L. Mandelli[94a], I. Mandić[78], J. Maneira[128a,128b], L. Manhaes de Andrade Filho[26b], J. Manjarres Ramos[163b], A. Mann[102], A. Manousos[32], B. Mansoulie[138], J. D. Mansour[35a], R. Mantifel[90], M. Mantoani[57], S. Manzoni[94a,94b], L. Mapelli[32], G. Marceca[29], L. March[52], G. Marchiori[83], M. Marcisovsky[129], M. Marjanovic[14], D. E. Marley[92], F. Marroquim[26a], S. P. Marsden[87], Z. Marshall[16], S. Marti-Garcia[170], B. Martin[93], T. A. Martin[173], V. J. Martin[49], B. Martin dit La tour[15], M. Martinez[13,t], V. I. Martinez Outschoorn[169], S. Martin-Haugh[133], V. S. Martoiu[28b], A. C. Martyniuk[81], A. Marzin[32], L. Masetti[86], T. Mashimo[157], R. Mashinistov[98], J. Masik[87], A. L. Maslennikov[111,c], I. Massa[22a,22b], L. Massa[22a,22b], P. Mastrandrea[5], A. Mastroberardino[40a,40b], T. Masubuchi[157], P. Mättig[178], J. Mattmann[86], J. Maurer[28b], S. J. Maxfield[77], D. A. Maximov[111,c], R. Mazini[153], I. Maznas[156], S. M. Mazza[94a,94b], N. C. Mc Fadden[107], G. Mc Goldrick[161], S. P. Mc Kee[92], A. McCarn[92], R. L. McCarthy[150], T. G. McCarthy[103], L. I. McClymont[81], E. F. McDonald[91], J. A. Mcfayden[81], G. Mchedlidze[57], S. J. McMahon[133], R. A. McPherson[172,n], M. Medinnis[45], S. Meehan[140], S. Mehlhase[102], A. Mehta[77], K. Meier[60a], C. Meineck[102], B. Meirose[44], D. Melini[170,ae], B. R. Mellado Garcia[147c], M. Melo[146a], F. Meloni[18], S. B. Menary[87], L. Meng[77], X. T. Meng[92], A. Mengarelli[22a,22b], S. Menke[103], E. Meoni[165], S. Mergelmeyer[17], P. Mermod[52], L. Merola[106a,106b], C. Meroni[94a], F. S. Merritt[33], A. Messina[134a,134b], J. Metcalfe[6], A. S. Mete[166], C. Meyer[86], C. Meyer[124], J-P. Meyer[138], J. Meyer[109], H. Meyer Zu Theenhausen[60a], F. Miano[151], R. P. Middleton[133], S. Miglioranzi[53a,53b], L. Mijović[49], G. Mikenberg[175], M. Mikestikova[129], M. Mikuž[78], M. Milesi[91], A. Milic[27], D. W. Miller[33], C. Mills[49], A. Milov[175], D. A. Milstead[148a,148b], A. A. Minaenko[132], Y. Minami[157], I. A. Minashvili[68], A. I. Mincer[112], B. Mindur[41a], M. Mineev[68], Y. Minegishi[157], Y. Ming[176], L. M. Mir[13], K. P. Mistry[124], T. Mitani[174], J. Mitrevski[102], V. A. Mitsou[170], A. Miucci[18], P. S. Miyagawa[141], A. Mizukami[69], J. U. Mjörnmark[84], M. Mlynarikova[131], T. Moa[148a,148b], K. Mochizuki[97], P. Mogg[51], S. Mohapatra[38], S. Molander[148a,148b], R. Moles-Valls[23], R. Monden[71], M. C. Mondragon[93], K. Mönig[45], J. Monk[39], E. Monnier[88], A. Montalbano[150], J. Montejo Berlingen[32], F. Monticelli[74], S. Monzani[94a,94b], R. W. Moore[3], N. Morange[119], D. Moreno[21], M. Moreno Llácer[57], P. Morettini[53a], S. Morgenstern[32], D. Mori[144], T. Mori[157], M. Morii[59], M. Morinaga[157], V. Morisbak[121], S. Moritz[86], A. K. Morley[152], G. Mornacchi[32], J. D. Morris[79], L. Morvaj[150], P. Moschovakos[10], M. Mosidze[54b], H. J. Moss[141], J. Moss[145,af], K. Motohashi[159], R. Mount[145], E. Mountricha[27], E. J. W. Moyse[89], S. Muanza[88], R. D. Mudd[19], F. Mueller[103], J. Mueller[127], R. S. P. Mueller[102], T. Mueller[30], D. Muenstermann[75], P. Mullen[56], G. A. Mullier[18], F. J. Munoz Sanchez[87], J. A. Murillo Quijada[19], W. J. Murray[173,133], H. Musheghyan[57], M. Muškinja[78], A. G. Myagkov[132,ag], M. Myska[130], B. P. Nachman[145], O. Nackenhorst[52], K. Nagai[122], R. Nagai[69,aa], K. Nagano[69], Y. Nagasaka[61], K. Nagata[164], M. Nagel[51], E. Nagy[88], A. M. Nairz[32], Y. Nakahama[105], K. Nakamura[69], T. Nakamura[157], I. Nakano[114], R. F. Naranjo Garcia[45], R. Narayan[11], D. I. Narrias Villar[60a], I. Naryshkin[125], T. Naumann[45], G. Navarro[21], R. Nayyar[7], H. A. Neal[92], P. Yu. Nechaeva[98], T. J. Neep[87], A. Negri[123a,123b], M. Negrini[22a], S. Nektarijevic[108], C. Nellist[119], A. Nelson[166], S. Nemecek[129], P. Nemethy[112], A. A. Nepomuceno[26a], M. Nessi[32,ah], M. S. Neubauer[169], M. Neumann[178], R. M. Neves[112], P. Nevski[27], P. R. Newman[19], D. H. Nguyen[6], T. Nguyen Manh[97], R. B. Nickerson[122], R. Nicolaidou[138], J. Nielsen[139], A. Nikiforov[17], V. Nikolaenko[132,ag], I. Nikolic-Audit[83], K. Nikolopoulos[19], J. K. Nilsen[121], P. Nilsson[27], Y. Ninomiya[157], A. Nisati[134a], R. Nisius[103], T. Nobe[157], M. Nomachi[120], I. Nomidis[31], T. Nooney[79], S. Norberg[115], M. Nordberg[32], N. Norjoharuddeen[122], O. Novgorodova[47], S. Nowak[103], M. Nozaki[69], L. Nozka[117], K. Ntekas[166], E. Nurse[81], F. Nuti[91], F. O'grady[7], D. C. O'Neil[144], A. A. O'Rourke[45], V. O'Shea[56], F. G. Oakham[31,d], H. Oberlack[103], T. Obermann[23], J. Ocariz[83], A. Ochi[70], I. Ochoa[38], J. P. Ochoa-Ricoux[34a], S. Oda[73], S. Odaka[69], H. Ogren[64], A. Oh[87], S. H. Oh[48], C. C. Ohm[16], H. Ohman[168], H. Oide[53a,53b], H. Okawa[164], Y. Okumura[157], T. Okuyama[69], A. Olariu[28b], L. F. Oleiro Seabra[128a], S. A. Olivares Pino[49], D. Oliveira Damazio[27], A. Olszewski[42], J. Olszowska[42], A. Onofre[128a,128e], K. Onogi[105], P. U. E. Onyisi[11,w], M. J. Oreglia[33], Y. Oren[155], D. Orestano[136a,136b], N. Orlando[62b], R. S. Orr[161], B. Osculati[53a,53b,*], R. Ospanov[87], G. Otero y Garzon[29], H. Otono[73], M. Ouchrif[137d], F. Ould-Saada[121], A. Ouraou[138], K. P. Oussoren[109], Q. Ouyang[35a], M. Owen[56], R. E. Owen[19], V. E. Ozcan[20a], N. Ozturk[8], K. Pachal[144], A. Pacheco Pages[13], L. Pacheco Rodriguez[138], C. Padilla Aranda[13], S. Pagan Griso[16], M. Paganini[179], F. Paige[27], P. Pais[89], K. Pajchel[121], G. Palacino[64], S. Palazzo[40a,40b], S. Palestini[32], M. Palka[41b], D. Pallin[37], E. St. Panagiotopoulou[10], I. Panagoulias[10], C. E. Pandini[83], J. G. Panduro Vazquez[80], P. Pani[148a,148b], S. Panitkin[27], D. Pantea[28b], L. Paolozzi[52], Th. D. Papadopoulou[10],

K. Papageorgiou[9], A. Paramonov[6], D. Paredes Hernandez[179], A. J. Parker[75], M. A. Parker[30], K. A. Parker[141], F. Parodi[53a,53b], J. A. Parsons[38], U. Parzefall[51], V. R. Pascuzzi[161], E. Pasqualucci[134a], S. Passaggio[53a], Fr. Pastore[80], G. Pásztor[31,ai], S. Pataraia[178], J. R. Pater[87], T. Pauly[32], J. Pearce[172], B. Pearson[115], L. E. Pedersen[39], S. Pedraza Lopez[170], R. Pedro[128a,128b], S. V. Peleganchuk[111,c], O. Penc[129], C. Peng[35a], H. Peng[36a], J. Penwell[64], B. S. Peralva[26b], M. M. Perego[138], D. V. Perepelitsa[27], E. Perez Codina[163a], L. Perini[94a,94b], H. Pernegger[32], S. Perrella[106a,106b], R. Peschke[45], V. D. Peshekhonov[68], K. Peters[45], R. F. Y. Peters[87], B. A. Petersen[32], T. C. Petersen[39], E. Petit[58], A. Petridis[1], C. Petridou[156], P. Petroff[119], E. Petrolo[134a], M. Petrov[122], F. Petrucci[136a,136b], N. E. Pettersson[89], A. Peyaud[138], R. Pezoa[34b], P. W. Phillips[133], G. Piacquadio[145,aj], E. Pianori[173], A. Picazio[89], E. Piccaro[79], M. Piccinini[22a,22b], M. A. Pickering[122], R. Piegaia[29], J. E. Pilcher[33], A. D. Pilkington[87], A. W. J. Pin[87], M. Pinamonti[167a,167c,ak], J. L. Pinfold[3], A. Pingel[39], S. Pires[83], H. Pirumov[45], M. Pitt[175], L. Plazak[146a], M.-A. Pleier[27], V. Pleskot[86], E. Plotnikova[68], D. Pluth[67], R. Poettgen[148a,148b], L. Poggioli[119], D. Pohl[23], G. Polesello[123a], A. Poley[45], A. Policicchio[40a,40b], R. Polifka[161], A. Polini[22a], C. S. Pollard[56], V. Polychronakos[27], K. Pommès[32], L. Pontecorvo[134a], B. G. Pope[93], G. A. Popeneciu[28c], A. Poppleton[32], S. Pospisil[130], K. Potamianos[16], I. N. Potrap[68], C. J. Potter[30], C. T. Potter[118], G. Poulard[32], J. Poveda[32], V. Pozdnyakov[68], M. E. Pozo Astigarraga[32], P. Pralavorio[88], A. Pranko[16], S. Prell[67], D. Price[87], L. E. Price[6], M. Primavera[76a], S. Prince[90], K. Prokofiev[62c], F. Prokoshin[34b], S. Protopopescu[27], J. Proudfoot[6], M. Przybycien[41a], D. Puddu[136a,136b], M. Purohit[27,al], P. Puzo[119], J. Qian[92], G. Qin[56], Y. Qin[87], A. Quadt[57], W. B. Quayle[167a,167b], M. Queitsch-Maitland[45], D. Quilty[56], S. Raddum[121], V. Radeka[27], V. Radescu[122], S. K. Radhakrishnan[150], P. Radloff[118], P. Rados[91], F. Ragusa[94a,94b], G. Rahal[181], J. A. Raine[87], S. Rajagopalan[27], M. Rammensee[32], C. Rangel-Smith[168], M. G. Ratti[94a,94b], D. M. Rauch[45], F. Rauscher[102], S. Rave[86], T. Ravenscroft[56], I. Ravinovich[175], M. Raymond[32], A. L. Read[121], N. P. Readioff[77], M. Reale[76a,76b], D. M. Rebuzzi[123a,123b], A. Redelbach[177], G. Redlinger[27], R. Reece[139], R. G. Reed[147c], K. Reeves[44], L. Rehnisch[17], J. Reichert[124], A. Reiss[86], C. Rembser[32], H. Ren[35a], M. Rescigno[134a], S. Resconi[94a], O. L. Rezanova[111,c], P. Reznicek[131], R. Rezvani[97], R. Richter[103], S. Richter[81], E. Richter-Was[41b], O. Ricken[23], M. Ridel[83], P. Rieck[17], C. J. Riegel[178], J. Rieger[57], O. Rifki[115], M. Rijssenbeek[150], A. Rimoldi[123a,123b], M. Rimoldi[18], L. Rinaldi[22a], B. Ristić[52], E. Ritsch[32], I. Riu[13], F. Rizatdinova[116], E. Rizvi[79], C. Rizzi[13], S. H. Robertson[90,n], A. Robichaud-Veronneau[90], D. Robinson[30], J. E. M. Robinson[45], A. Robson[56], C. Roda[126a,126b], Y. Rodina[88,am], A. Rodriguez Perez[13], D. Rodriguez Rodriguez[170], S. Roe[32], C. S. Rogan[59], O. Røhne[121], J. Roloff[59], A. Romaniouk[100], M. Romano[22a,22b], S. M. Romano Saez[37], E. Romero Adam[170], N. Rompotis[140], M. Ronzani[51], L. Roos[83], E. Ros[170], S. Rosati[134a], K. Rosbach[51], P. Rose[139], N.-A. Rosien[57], V. Rossetti[148a,148b], E. Rossi[106a,106b], L. P. Rossi[53a], J. H. N. Rosten[30], R. Rosten[140], M. Rotaru[28b], I. Roth[175], J. Rothberg[140], D. Rousseau[119], A. Rozanov[88], Y. Rozen[154], X. Ruan[147c], F. Rubbo[145], M. S. Rudolph[161], F. Rühr[51], A. Ruiz-Martinez[31], Z. Rurikova[51], N. A. Rusakovich[68], A. Ruschke[102], H. L. Russell[140], J. P. Rutherfoord[7], N. Ruthmann[32], Y. F. Ryabov[125], M. Rybar[169], G. Rybkin[119], S. Ryu[6], A. Ryzhov[132], G. F. Rzehorz[57], A. F. Saavedra[152], G. Sabato[109], S. Sacerdoti[29], H. F-W. Sadrozinski[139], R. Sadykov[68], F. Safai Tehrani[134a], P. Saha[110], M. Sahinsoy[60a], M. Saimpert[138], T. Saito[157], H. Sakamoto[157], Y. Sakurai[174], G. Salamanna[136a,136b], A. Salamon[135a,135b], J. E. Salazar Loyola[34b], D. Salek[109], P. H. Sales De Bruin[140], D. Salihagic[103], A. Salnikov[145], J. Salt[170], D. Salvatore[40a,40b], F. Salvatore[151], A. Salvucci[62a,62b,62c], A. Salzburger[32], D. Sammel[51], D. Sampsonidis[156], J. Sánchez[170], V. Sanchez Martinez[170], A. Sanchez Pineda[106a,106b], H. Sandaker[121], R. L. Sandbach[79], M. Sandhoff[178], C. Sandoval[21], D. P. C. Sankey[133], M. Sannino[53a,53b], A. Sansoni[50], C. Santoni[37], R. Santonico[135a,135b], H. Santos[128a], I. Santoyo Castillo[151], K. Sapp[127], A. Sapronov[68], J. G. Saraiva[128a,128d], B. Sarrazin[23], O. Sasaki[69], K. Sato[164], E. Sauvan[5], G. Savage[80], P. Savard[161,d], N. Savic[103], C. Sawyer[133], L. Sawyer[82,s], J. Saxon[33], C. Sbarra[22a], A. Sbrizzi[22a,22b], T. Scanlon[81], D. A. Scannicchio[166], M. Scarcella[152], V. Scarfone[40a,40b], J. Schaarschmidt[175], P. Schacht[103], B. M. Schachtner[102], D. Schaefer[32], L. Schaefer[124], R. Schaefer[45], J. Schaeffer[86], S. Schaepe[23], S. Schaetzel[60b], U. Schäfer[86], A. C. Schaffer[119], D. Schaile[102], R. D. Schamberger[150], V. Scharf[60a], V. A. Schegelsky[125], D. Scheirich[131], M. Schernau[166], C. Schiavi[53a,53b], S. Schier[139], C. Schillo[51], M. Schioppa[40a,40b], S. Schlenker[32], K. R. Schmidt-Sommerfeld[103], K. Schmieden[32], C. Schmitt[86], S. Schmitt[45], S. Schmitz[86], B. Schneider[163a], U. Schnoor[51], L. Schoeffel[138], A. Schoening[60b], B. D. Schoenrock[93], E. Schopf[23], M. Schott[86], J. F. P. Schouwenberg[108], J. Schovancova[8], S. Schramm[52], M. Schreyer[177], N. Schuh[86], A. Schulte[86], M. J. Schultens[23], H.-C. Schultz-Coulon[60a], H. Schulz[17], M. Schumacher[51], B. A. Schumm[139], Ph. Schune[138], A. Schwartzman[145], T. A. Schwarz[92], H. Schweiger[87], Ph. Schwemling[138], R. Schwienhorst[93], J. Schwindling[138], T. Schwindt[23], G. Sciolla[25], F. Scuri[126a,126b], F. Scutti[91], J. Searcy[92], P. Seema[23], S. C. Seidel[107], A. Seiden[139], F. Seifert[130], J. M. Seixas[26a], G. Sekhniaidze[106a], K. Sekhon[92], S. J. Sekula[43], D. M. Seliverstov[125,*], N. Semprini-Cesari[22a,22b], C. Serfon[121], L. Serin[119], L. Serkin[167a,167b], M. Sessa[136a,136b], R. Seuster[172], H. Severini[115], T. Sfiligoj[78], F. Sforza[32], A. Sfyrla[52], E. Shabalina[57], N. W. Shaikh[148a,148b], L. Y. Shan[35a], R. Shang[169], J. T. Shank[24], M. Shapiro[16], P. B. Shatalov[99], K. Shaw[167a,167b], S. M. Shaw[87], A. Shcherbakova[148a,148b], C. Y. Shehu[151], P. Sherwood[81], L. Shi[153,an], S. Shimizu[70], C. O. Shimmin[166], M. Shimojima[104],

S. Shirabe[73], M. Shiyakova[68,ao], A. Shmeleva[98], D. Shoaleh Saadi[97], M. J. Shochet[33], S. Shojaii[94a], D. R. Shope[115], S. Shrestha[113], E. Shulga[100], M. A. Shupe[7], P. Sicho[129], A. M. Sickles[169], P. E. Sidebo[149], E. Sideras Haddad[147c], O. Sidiropoulou[177], D. Sidorov[116], A. Sidoti[22a,22b], F. Siegert[47], Dj. Sijacki[14], J. Silva[128a,128d], S. B. Silverstein[148a], V. Simak[130], Lj. Simic[14], S. Simion[119], E. Simioni[86], B. Simmons[81], D. Simon[37], M. Simon[86], P. Sinervo[161], N. B. Sinev[118], M. Sioli[22a,22b], G. Siragusa[177], S. Yu. Sivoklokov[101], J. Sjölin[148a,148b], M. B. Skinner[75], H. P. Skottowe[59], P. Skubic[115], M. Slater[19], T. Slavicek[130], M. Slawinska[109], K. Sliwa[165], R. Slovak[131], V. Smakhtin[175], B. H. Smart[5], L. Smestad[15], J. Smiesko[146a], S. Yu. Smirnov[100], Y. Smirnov[100], L. N. Smirnova[101,ap], O. Smirnova[84], J. W. Smith[57], M. N. K. Smith[38], R. W. Smith[38], M. Smizanska[75], K. Smolek[130], A. A. Snesarev[98], I. M. Snyder[118], S. Snyder[27], R. Sobie[172,n], F. Socher[47], A. Soffer[155], D. A. Soh[153], G. Sokhrannyi[78], C. A. Solans Sanchez[32], M. Solar[130], E. Yu. Soldatov[100], U. Soldevila[170], A. A. Solodkov[132], A. Soloshenko[68], O. V. Solovyanov[132], V. Solovyev[125], P. Sommer[51], H. Son[165], H. Y. Song[36a,aq], A. Sood[16], A. Sopczak[130], V. Sopko[130], V. Sorin[13], D. Sosa[60b], C. L. Sotiropoulou[126a,126b], R. Soualah[167a,167c], A. M. Soukharev[111,c], D. South[45], B. C. Sowden[80], S. Spagnolo[76a,76b], M. Spalla[126a,126b], M. Spangenberg[173], F. Spanò[80], D. Sperlich[17], F. Spettel[103], R. Spighi[22a], G. Spigo[32], L. A. Spiller[91], M. Spousta[131], R. D. St. Denis[56,*], A. Stabile[94a], R. Stamen[60a], S. Stamm[17], E. Stanecka[42], R. W. Stanek[6], C. Stanescu[136a], M. Stanescu-Bellu[45], M. M. Stanitzki[45], S. Stapnes[121], E. A. Starchenko[132], G. H. Stark[33], J. Stark[58], S. H Stark[39], P. Staroba[129], P. Starovoitov[60a], S. Stärz[32], R. Staszewski[42], P. Steinberg[27], B. Stelzer[144], H. J. Stelzer[32], O. Stelzer-Chilton[163a], H. Stenzel[55], G. A. Stewart[56], J. A. Stillings[23], M. C. Stockton[90], M. Stoebe[90], G. Stoicea[28b], P. Stolte[57], S. Stonjek[103], A. R. Stradling[8], A. Straessner[47], M. E. Stramaglia[18], J. Strandberg[149], S. Strandberg[148a,148b], A. Strandlie[121], M. Strauss[115], P. Strizenec[146b], R. Ströhmer[177], D. M. Strom[118], R. Stroynowski[43], A. Strubig[108], S. A. Stucci[27], B. Stugu[15], N. A. Styles[45], D. Su[145], J. Su[127], S. Suchek[60a], Y. Sugaya[120], M. Suk[130], V. V. Sulin[98], S. Sultansoy[4c], T. Sumida[71], S. Sun[59], X. Sun[35a], J. E. Sundermann[51], K. Suruliz[151], C. J. E. Suster[152], M. R. Sutton[151], S. Suzuki[69], M. Svatos[129], M. Swiatlowski[33], S. P. Swift[2], I. Sykora[146a], T. Sykora[131], D. Ta[51], C. Taccini[136a,136b], K. Tackmann[45], J. Taenzer[161], A. Taffard[166], R. Tafirout[163a], N. Taiblum[155], H. Takai[27], R. Takashima[72], T. Takeshita[142], Y. Takubo[69], M. Talby[88], A. A. Talyshev[111,c], K. G. Tan[91], J. Tanaka[157], M. Tanaka[159], R. Tanaka[119], S. Tanaka[69], R. Tanioka[70], B. B. Tannenwald[113], S. Tapia Araya[34b], S. Tapprogge[86], S. Tarem[154], G. F. Tartarelli[94a], P. Tas[131], M. Tasevsky[129], T. Tashiro[71], E. Tassi[40a,40b], A. Tavares Delgado[128a,128b], Y. Tayalati[137e], A. C. Taylor[107], G. N. Taylor[91], P. T. E. Taylor[91], W. Taylor[163b], F. A. Teischinger[32], P. Teixeira-Dias[80], K. K. Temming[51], D. Temple[144], H. Ten Kate[32], P. K. Teng[153], J. J. Teoh[120], F. Tepel[178], S. Terada[69], K. Terashi[157], J. Terron[85], S. Terzo[13], M. Testa[50], R. J. Teuscher[161,n], T. Theveneaux-Pelzer[88], J. P. Thomas[19], J. Thomas-Wilsker[80], P. D. Thompson[19], A. S. Thompson[56], L. A. Thomsen[179], E. Thomson[124], M. J. Tibbetts[16], R. E. Ticse Torres[88], V. O. Tikhomirov[98,ar], Yu. A. Tikhonov[111,c], S. Timoshenko[100], P. Tipton[179], S. Tisserant[88], K. Todome[159], T. Todorov[5,*], S. Todorova-Nova[131], J. Tojo[73], S. Tokár[146a], K. Tokushuku[69], E. Tolley[59], L. Tomlinson[87], M. Tomoto[105], L. Tompkins[145,as], K. Toms[107], B. Tong[59], P. Tornambe[51], E. Torrence[118], H. Torres[144], E. Torró Pastor[140], J. Toth[88,at], F. Touchard[88], D. R. Tovey[141], T. Trefzger[177], A. Tricoli[27], I. M. Trigger[163a], S. Trincaz-Duvoid[83], M. F. Tripiana[13], W. Trischuk[161], B. Trocmé[58], A. Trofymov[45], C. Troncon[94a], M. Trottier-McDonald[16], M. Trovatelli[172], L. Truong[167a,167c], M. Trzebinski[42], A. Trzupek[42], J. C-L. Tseng[122], P. V. Tsiareshka[95], G. Tsipolitis[10], N. Tsirintanis[9], S. Tsiskaridze[13], V. Tsiskaridze[51], E. G. Tskhadadze[54a], K. M. Tsui[62a], I. I. Tsukerman[99], V. Tsulaia[16], S. Tsuno[69], D. Tsybychev[150], Y. Tu[62b], A. Tudorache[28b], V. Tudorache[28b], T. T. Tulbure[28a], A. N. Tuna[59], S. A. Tupputi[22a,22b], S. Turchikhin[68], D. Turgeman[175], I. Turk Cakir[4b,au], R. Turra[94a,94b], P. M. Tuts[38], G. Ucchielli[22a,22b], I. Ueda[157], M. Ughetto[148a,148b], F. Ukegawa[164], G. Unal[32], A. Undrus[27], G. Unel[166], F. C. Ungaro[91], Y. Unno[69], C. Unverdorben[102], J. Urban[146b], P. Urquijo[91], P. Urrejola[86], G. Usai[8], J. Usui[69], L. Vacavant[88], V. Vacek[130], B. Vachon[90], C. Valderanis[102], E. Valdes Santurio[148a,148b], N. Valencic[109], S. Valentinetti[22a,22b], A. Valero[170], L. Valery[13], S. Valkar[131], J. A. Valls Ferrer[170], W. Van Den Wollenberg[109], P. C. Van Der Deijl[109], H. van der Graaf[109], N. van Eldik[154], P. van Gemmeren[6], J. Van Nieuwkoop[144], I. van Vulpen[109], M. C. van Woerden[109], M. Vanadia[134a,134b], W. Vandelli[32], R. Vanguri[124], A. Vaniachine[160], P. Vankov[109], G. Vardanyan[180], R. Vari[134a], E. W. Varnes[7], T. Varol[43], D. Varouchas[83], A. Vartapetian[8], K. E. Varvell[152], J. G. Vasquez[179], G. A. Vasquez[34b], F. Vazeille[37], T. Vazquez Schroeder[90], J. Veatch[57], V. Veeraraghavan[7], L. M. Veloce[161], F. Veloso[128a,128c], S. Veneziano[134a], A. Ventura[76a,76b], M. Venturi[172], N. Venturi[161], A. Venturini[25], V. Vercesi[123a], M. Verducci[134a,134b], W. Verkerke[109], J. C. Vermeulen[109], A. Vest[47,av], M. C. Vetterli[144,d], O. Viazlo[84], I. Vichou[169,*], T. Vickey[141], O. E. Vickey Boeriu[141], G. H. A. Viehhauser[122], S. Viel[16], L. Vigani[122], M. Villa[22a,22b], M. Villaplana Perez[94a,94b], E. Vilucchi[50], M. G. Vincter[31], V. B. Vinogradov[68], C. Vittori[22a,22b], I. Vivarelli[151], S. Vlachos[10], M. Vlasak[130], M. Vogel[178], P. Vokac[130], G. Volpi[126a,126b], M. Volpi[91], H. von der Schmitt[103], E. von Toerne[23], V. Vorobel[131], K. Vorobev[100], M. Vos[170], R. Voss[32], J. H. Vossebeld[77], N. Vranjes[14], M. Vranjes Milosavljevic[14], V. Vrba[129], M. Vreeswijk[109], R. Vuillermet[32], I. Vukotic[33], P. Wagner[23], W. Wagner[178], H. Wahlberg[74], S. Wahrmund[47], J. Wakabayashi[105], J. Walder[75], R. Walker[102], W. Walkowiak[143], V. Wallangen[148a,148b], C. Wang[35b], C. Wang[36b,aw], F. Wang[176], H. Wang[16], H. Wang[43], J. Wang[45], J. Wang[152], K. Wang[90],

R. Wang[6], S. M. Wang[153], T. Wang[38], W. Wang[36a], C. Wanotayaroj[118], A. Warburton[90], C. P. Ward[30], D. R. Wardrope[81], A. Washbrook[49], P. M. Watkins[19], A. T. Watson[19], M. F. Watson[19], G. Watts[140], S. Watts[87], B. M. Waugh[81], S. Webb[86], M. S. Weber[18], S. W. Weber[177], S. A. Weber[31], J. S. Webster[6], A. R. Weidberg[122], B. Weinert[64], J. Weingarten[57], C. Weiser[51], H. Weits[109], P. S. Wells[32], T. Wenaus[27], T. Wengler[32], S. Wenig[32], N. Wermes[23], M. D. Werner[67], P. Werner[32], M. Wessels[60a], J. Wetter[165], K. Whalen[118], N. L. Whallon[140], A. M. Wharton[75], A. White[8], M. J. White[1], R. White[34b], D. Whiteson[166], F. J. Wickens[133], W. Wiedenmann[176], M. Wielers[133], C. Wiglesworth[39], L. A. M. Wiik-Fuchs[23], A. Wildauer[103], F. Wilk[87], H. G. Wilkens[32], H. H. Williams[124], S. Williams[109], C. Willis[93], S. Willocq[89], J. A. Wilson[19], I. Wingerter-Seez[5], F. Winklmeier[118], O. J. Winston[151], B. T. Winter[23], M. Wittgen[145], T. M. H. Wolf[109], R. Wolff[88], M. W. Wolter[42], H. Wolters[128a,128c], S. D. Worm[133], B. K. Wosiek[42], J. Wotschack[32], M. J. Woudstra[87], K. W. Wozniak[42], M. Wu[58], M. Wu[33], S. L. Wu[176], X. Wu[52], Y. Wu[92], T. R. Wyatt[87], B. M. Wynne[49], S. Xella[39], Z. Xi[92], D. Xu[35a], L. Xu[27], B. Yabsley[152], S. Yacoob[147a], D. Yamaguchi[159], Y. Yamaguchi[120], A. Yamamoto[69], S. Yamamoto[157], T. Yamanaka[157], K. Yamauchi[105], Y. Yamazaki[70], Z. Yan[24], H. Yang[36c], H. Yang[176], Y. Yang[153], Z. Yang[15], W-M. Yao[16], Y. C. Yap[83], Y. Yasu[69], E. Yatsenko[5], K. H. Yau Wong[23], J. Ye[43], S. Ye[27], I. Yeletskikh[68], E. Yildirim[86], K. Yorita[174], R. Yoshida[6], K. Yoshihara[124], C. Young[145], C. J. S. Young[32], S. Youssef[24], D. R. Yu[16], J. Yu[8], J. M. Yu[92], J. Yu[67], L. Yuan[70], S. P. Y. Yuen[23], I. Yusuff[30,ax], B. Zabinski[42], G. Zacharis[10], R. Zaidan[66], A. M. Zaitsev[132,ag], N. Zakharchuk[45], J. Zalieckas[15], A. Zaman[150], S. Zambito[59], L. Zanello[134a,134b], D. Zanzi[91], C. Zeitnitz[178], M. Zeman[130], A. Zemla[41a], J. C. Zeng[169], Q. Zeng[145], O. Zenin[132], T. Ženiš[146a], D. Zerwas[119], D. Zhang[92], F. Zhang[176], G. Zhang[36a,aq], H. Zhang[35b], J. Zhang[6], L. Zhang[51], L. Zhang[36a], M. Zhang[169], R. Zhang[23], R. Zhang[36a,aw], X. Zhang[36b], Z. Zhang[119], X. Zhao[43], Y. Zhao[36b,ay], Z. Zhao[36a], A. Zhemchugov[68], J. Zhong[122], B. Zhou[92], C. Zhou[176], L. Zhou[38], L. Zhou[43], M. Zhou[150], N. Zhou[35c], C. G. Zhu[36b], H. Zhu[35a], J. Zhu[92], Y. Zhu[36a], X. Zhuang[35a], K. Zhukov[98], A. Zibell[177], D. Zieminska[64], N. I. Zimine[68], C. Zimmermann[86], S. Zimmermann[51], Z. Zinonos[57], M. Zinser[86], M. Ziolkowski[143], L. Živković[14], G. Zobernig[176], A. Zoccoli[22a,22b], M. zur Nedden[17], L. Zwalinski[32]

[1] Department of Physics, University of Adelaide, Adelaide, SA, Australia
[2] Physics Department, SUNY Albany, Albany, NY, USA
[3] Department of Physics, University of Alberta, Edmonton, AB, Canada
[4] [(a)]Department of Physics, Ankara University, Ankara, Turkey; [(b)]Istanbul Aydin University, Istanbul, Turkey; [(c)]Division of Physics, TOBB University of Economics and Technology, Ankara, Turkey
[5] LAPP, CNRS/IN2P3 and Université Savoie Mont Blanc, Annecy-le-Vieux, France
[6] High Energy Physics Division, Argonne National Laboratory, Argonne, IL, USA
[7] Department of Physics, University of Arizona, Tucson, AZ, USA
[8] Department of Physics, The University of Texas at Arlington, Arlington, TX, USA
[9] Physics Department, National and Kapodistrian University of Athens, Athens, Greece
[10] Physics Department, National Technical University of Athens, Zografou, Greece
[11] Department of Physics, The University of Texas at Austin, Austin, TX, USA
[12] Institute of Physics, Azerbaijan Academy of Sciences, Baku, Azerbaijan
[13] Institut de Física d'Altes Energies (IFAE), The Barcelona Institute of Science and Technology, Barcelona, Spain
[14] Institute of Physics, University of Belgrade, Belgrade, Serbia
[15] Department for Physics and Technology, University of Bergen, Bergen, Norway
[16] Physics Division, Lawrence Berkeley National Laboratory and University of California, Berkeley, CA, USA
[17] Department of Physics, Humboldt University, Berlin, Germany
[18] Albert Einstein Center for Fundamental Physics and Laboratory for High Energy Physics, University of Bern, Bern, Switzerland
[19] School of Physics and Astronomy, University of Birmingham, Birmingham, UK
[20] [(a)]Department of Physics, Bogazici University, Istanbul, Turkey; [(b)]Department of Physics Engineering, Gaziantep University, Gaziantep, Turkey; [(c)]Faculty of Engineering and Natural Sciences, Istanbul Bilgi University, Istanbul, Turkey; [(d)]Faculty of Engineering and Natural Sciences, Bahcesehir University, Istanbul, Turkey
[21] Centro de Investigaciones, Universidad Antonio Narino, Bogota, Colombia
[22] [(a)]INFN Sezione di Bologna, Bologna, Italy; [(b)]Dipartimento di Fisica e Astronomia, Università di Bologna, Bologna, Italy
[23] Physikalisches Institut, University of Bonn, Bonn, Germany
[24] Department of Physics, Boston University, Boston, MA, USA
[25] Department of Physics, Brandeis University, Waltham, MA, USA

[26] [(a)]Universidade Federal do Rio De Janeiro COPPE/EE/IF, Rio de Janeiro, Brazil; [(b)]Electrical Circuits Department, Federal University of Juiz de Fora (UFJF), Juiz de Fora, Brazil; [(c)]Federal University of Sao Joao del Rei (UFSJ), Sao Joao del Rei, Brazil; [(d)]Instituto de Fisica, Universidade de Sao Paulo, Sao Paulo, Brazil
[27] Physics Department, Brookhaven National Laboratory, Upton, NY, USA
[28] [(a)]Transilvania University of Brasov, Brasov, Romania; [(b)]Horia Hulubei National Institute of Physics and Nuclear Engineering, Bucharest, Romania; [(c)]Physics Department, National Institute for Research and Development of Isotopic and Molecular Technologies, Cluj-Napoca, Romania; [(d)]University Politehnica Bucharest, Bucharest, Romania; [(e)]West University in Timisoara, Timisoara, Romania
[29] Departamento de Física, Universidad de Buenos Aires, Buenos Aires, Argentina
[30] Cavendish Laboratory, University of Cambridge, Cambridge, UK
[31] Department of Physics, Carleton University, Ottawa, ON, Canada
[32] CERN, Geneva, Switzerland
[33] Enrico Fermi Institute, University of Chicago, Chicago, IL, USA
[34] [(a)]Departamento de Física, Pontificia Universidad Católica de Chile, Santiago, Chile; [(b)]Departamento de Física, Universidad Técnica Federico Santa María, Valparaíso, Chile
[35] [(a)]Institute of High Energy Physics, Chinese Academy of Sciences, Beijing, China; [(b)]Department of Physics, Nanjing University, Nanjing, Jiangsu, China; [(c)]Physics Department, Tsinghua University, Beijing 100084, China
[36] [(a)]Department of Modern Physics, University of Science and Technology of China, Anhui, China; [(b)]School of Physics, Shandong University, Shandong, China; [(c)]Department of Physics and Astronomy, Key Laboratory for Particle Physics, Astrophysics and Cosmology,Ministry of Education,Shanghai Key Laboratory for Particle Physics and Cosmology, Shanghai Jiao Tong University (also at PKU-CHEP), Shanghai, China
[37] Laboratoire de Physique Corpusculaire, Université Clermont Auvergne, Université Blaise Pascal, CNRS/IN2P3, Clermont-Ferrand, France
[38] Nevis Laboratory, Columbia University, Irvington, NY, USA
[39] Niels Bohr Institute, University of Copenhagen, Kobenhavn, Denmark
[40] [(a)]INFN Gruppo Collegato di Cosenza, Laboratori Nazionali di Frascati, Frascati, Italy; [(b)]Dipartimento di Fisica, Università della Calabria, Rende, Italy
[41] [(a)]Faculty of Physics and Applied Computer Science, AGH University of Science and Technology, Kraków, Poland; [(b)]Marian Smoluchowski Institute of Physics, Jagiellonian University, Krakow, Poland
[42] Institute of Nuclear Physics Polish Academy of Sciences, Krakow, Poland
[43] Physics Department, Southern Methodist University, Dallas, TX, USA
[44] Physics Department, University of Texas at Dallas, Richardson, TX, USA
[45] DESY, Hamburg and Zeuthen, Germany
[46] Lehrstuhl für Experimentelle Physik IV, Technische Universität Dortmund, Dortmund, Germany
[47] Institut für Kern- und Teilchenphysik, Technische Universität Dresden, Dresden, Germany
[48] Department of Physics, Duke University, Durham, NC, USA
[49] SUPA-School of Physics and Astronomy, University of Edinburgh, Edinburgh, UK
[50] INFN Laboratori Nazionali di Frascati, Frascati, Italy
[51] Fakultät für Mathematik und Physik, Albert-Ludwigs-Universität, Freiburg, Germany
[52] Departement de Physique Nucleaire et Corpusculaire, Université de Genève, Geneva, Switzerland
[53] [(a)]INFN Sezione di Genova, Genoa, Italy; [(b)]Dipartimento di Fisica, Università di Genova, Genova, Italy
[54] [(a)]E. Andronikashvili Institute of Physics, Iv. Javakhishvili Tbilisi State University, Tbilisi, Georgia; [(b)]High Energy Physics Institute, Tbilisi State University, Tbilisi, Georgia
[55] II Physikalisches Institut, Justus-Liebig-Universität Giessen, Giessen, Germany
[56] SUPA-School of Physics and Astronomy, University of Glasgow, Glasgow, UK
[57] II Physikalisches Institut, Georg-August-Universität, Göttingen, Germany
[58] Laboratoire de Physique Subatomique et de Cosmologie, Université Grenoble-Alpes, CNRS/IN2P3, Grenoble, France
[59] Laboratory for Particle Physics and Cosmology, Harvard University, Cambridge, MA, USA
[60] [(a)]Kirchhoff-Institut für Physik, Ruprecht-Karls-Universität Heidelberg, Heidelberg, Germany; [(b)]Physikalisches Institut, Ruprecht-Karls-Universität Heidelberg, Heidelberg, Germany; [(c)]ZITI Institut für technische Informatik, Ruprecht-Karls-Universität Heidelberg, Mannheim, Germany
[61] Faculty of Applied Information Science, Hiroshima Institute of Technology, Hiroshima, Japan

[62] [(a)]Department of Physics, The Chinese University of Hong Kong, Shatin, NT, Hong Kong; [(b)]Department of Physics, The University of Hong Kong, Hong Kong, China; [(c)]Department of Physics and Institute for Advanced Study, The Hong Kong University of Science and Technology, Clear Water Bay, Kowloon, Hong Kong, China
[63] Department of Physics, National Tsing Hua University, Taiwan, Taiwan
[64] Department of Physics, Indiana University, Bloomington, IN, USA
[65] Institut für Astro- und Teilchenphysik, Leopold-Franzens-Universität, Innsbruck, Austria
[66] University of Iowa, Iowa city, IA, USA
[67] Department of Physics and Astronomy, Iowa State University, Ames, IA, USA
[68] Joint Institute for Nuclear Research, JINR Dubna, Dubna, Russia
[69] KEK, High Energy Accelerator Research Organization, Tsukuba, Japan
[70] Graduate School of Science, Kobe University, Kobe, Japan
[71] Faculty of Science, Kyoto University, Kyoto, Japan
[72] Kyoto University of Education, Kyoto, Japan
[73] Department of Physics, Kyushu University, Fukuoka, Japan
[74] Instituto de Física La Plata, Universidad Nacional de La Plata and CONICET, La Plata, Argentina
[75] Physics Department, Lancaster University, Lancaster, UK
[76] [(a)]INFN Sezione di Lecce, Lecce, Italy; [(b)]Dipartimento di Matematica e Fisica, Università del Salento, Lecce, Italy
[77] Oliver Lodge Laboratory, University of Liverpool, Liverpool, UK
[78] Department of Experimental Particle Physics, Jožef Stefan Institute and Department of Physics, University of Ljubljana, Ljubljana, Slovenia
[79] School of Physics and Astronomy, Queen Mary University of London, London, UK
[80] Department of Physics, Royal Holloway University of London, Surrey, UK
[81] Department of Physics and Astronomy, University College London, London, UK
[82] Louisiana Tech University, Ruston, LA, USA
[83] Laboratoire de Physique Nucléaire et de Hautes Energies, UPMC and Université Paris-Diderot and CNRS/IN2P3, Paris, France
[84] Fysiska institutionen, Lunds universitet, Lund, Sweden
[85] Departamento de Fisica Teorica C-15, Universidad Autonoma de Madrid, Madrid, Spain
[86] Institut für Physik, Universität Mainz, Mainz, Germany
[87] School of Physics and Astronomy, University of Manchester, Manchester, UK
[88] CPPM, Aix-Marseille Université and CNRS/IN2P3, Marseille, France
[89] Department of Physics, University of Massachusetts, Amherst, MA, USA
[90] Department of Physics, McGill University, Montreal, QC, Canada
[91] School of Physics, University of Melbourne, Melbourne, VIC, Australia
[92] Department of Physics, The University of Michigan, Ann Arbor, MI, USA
[93] Department of Physics and Astronomy, Michigan State University, East Lansing, MI, USA
[94] [(a)]INFN Sezione di Milano, Milan, Italy; [(b)]Dipartimento di Fisica, Università di Milano, Milano, Italy
[95] B.I. Stepanov Institute of Physics, National Academy of Sciences of Belarus, Minsk, Republic of Belarus
[96] Research Institute for Nuclear Problems of Byelorussian State University, Minsk, Republic of Belarus
[97] Group of Particle Physics, University of Montreal, Montreal, QC, Canada
[98] P.N. Lebedev Physical Institute of the Russian Academy of Sciences, Moscow, Russia
[99] Institute for Theoretical and Experimental Physics (ITEP), Moscow, Russia
[100] National Research Nuclear University MEPhI, Moscow, Russia
[101] D.V. Skobeltsyn Institute of Nuclear Physics, M.V. Lomonosov Moscow State University, Moscow, Russia
[102] Fakultät für Physik, Ludwig-Maximilians-Universität München, München, Germany
[103] Max-Planck-Institut für Physik (Werner-Heisenberg-Institut), München, Germany
[104] Nagasaki Institute of Applied Science, Nagasaki, Japan
[105] Graduate School of Science and Kobayashi-Maskawa Institute, Nagoya University, Nagoya, Japan
[106] [(a)]INFN Sezione di Napoli, Napoli, Italy; [(b)]Dipartimento di Fisica, Università di Napoli, Napoli, Italy
[107] Department of Physics and Astronomy, University of New Mexico, Albuquerque, NM, USA
[108] Institute for Mathematics, Astrophysics and Particle Physics, Radboud University Nijmegen/Nikhef, Nijmegen, Netherlands
[109] Nikhef National Institute for Subatomic Physics and University of Amsterdam, Amsterdam, Netherlands

[110] Department of Physics, Northern Illinois University, DeKalb, IL, USA
[111] Budker Institute of Nuclear Physics, SB RAS, Novosibirsk, Russia
[112] Department of Physics, New York University, New York, NY, USA
[113] Ohio State University, Columbus, OH, USA
[114] Faculty of Science, Okayama University, Okayama, Japan
[115] Homer L. Dodge Department of Physics and Astronomy, University of Oklahoma, Norman, OK, USA
[116] Department of Physics, Oklahoma State University, Stillwater, OK, USA
[117] Palacký University, RCPTM, Olomouc, Czech Republic
[118] Center for High Energy Physics, University of Oregon, Eugene, OR, USA
[119] LAL, University of Paris-Sud, CNRS/IN2P3, Université Paris-Saclay, Orsay, France
[120] Graduate School of Science, Osaka University, Osaka, Japan
[121] Department of Physics, University of Oslo, Oslo, Norway
[122] Department of Physics, Oxford University, Oxford, UK
[123] [(a)]INFN Sezione di Pavia, Pavia, Italy; [(b)]Dipartimento di Fisica, Università di Pavia, Pavia, Italy
[124] Department of Physics, University of Pennsylvania, Philadelphia, PA, USA
[125] National Research Centre "Kurchatov Institute" B.P. Konstantinov Petersburg Nuclear Physics Institute, St. Petersburg, Russia
[126] [(a)]INFN Sezione di Pisa, Pisa, Italy; [(b)]Dipartimento di Fisica E. Fermi, Università di Pisa, Pisa, Italy
[127] Department of Physics and Astronomy, University of Pittsburgh, Pittsburgh, PA, USA
[128] [(a)]Laboratório de Instrumentação e Física Experimental de Partículas-LIP, Lisboa, Portugal; [(b)]Faculdade de Ciências, Universidade de Lisboa, Lisboa, Portugal; [(c)]Department of Physics, University of Coimbra, Coimbra, Portugal; [(d)]Centro de Física Nuclear da Universidade de Lisboa, Lisboa, Portugal; [(e)]Departamento de Fisica, Universidade do Minho, Braga, Portugal; [(f)]Departamento de Fisica Teorica y del Cosmos and CAFPE, Universidad de Granada, Granada, Spain; [(g)]Dep Fisica and CEFITEC of Faculdade de Ciencias e Tecnologia, Universidade Nova de Lisboa, Caparica, Portugal
[129] Institute of Physics, Academy of Sciences of the Czech Republic, Praha, Czech Republic
[130] Czech Technical University in Prague, Praha, Czech Republic
[131] Charles University, Faculty of Mathematics and Physics, Prague, Czech Republic
[132] State Research Center Institute for High Energy Physics (Protvino), NRC KI, Moscow, Russia
[133] Particle Physics Department, Rutherford Appleton Laboratory, Didcot, UK
[134] [(a)]INFN Sezione di Roma, Roma, Italy; [(b)]Dipartimento di Fisica, Sapienza Università di Roma, Roma, Italy
[135] [(a)]INFN Sezione di Roma Tor Vergata, Roma, Italy; [(b)]Dipartimento di Fisica, Università di Roma Tor Vergata, Roma, Italy
[136] [(a)]INFN Sezione di Roma Tre, Roma, Italy; [(b)]Dipartimento di Matematica e Fisica, Università Roma Tre, Roma, Italy
[137] [(a)]Faculté des Sciences Ain Chock, Réseau Universitaire de Physique des Hautes Energies-Université Hassan II, Casablanca, Morocco; [(b)]Centre National de l'Energie des Sciences Techniques Nucleaires, Rabat, Morocco; [(c)]Faculté des Sciences Semlalia, Université Cadi Ayyad, LPHEA-Marrakech, Marrakech, Morocco; [(d)]Faculté des Sciences, Université Mohamed Premier and LPTPM, Oujda, Morocco; [(e)]Faculté des Sciences, Université Mohammed V, Rabat, Morocco
[138] DSM/IRFU (Institut de Recherches sur les Lois Fondamentales de l'Univers), CEA Saclay (Commissariat à l'Energie Atomique et aux Energies Alternatives), Gif-sur-Yvette, France
[139] Santa Cruz Institute for Particle Physics, University of California Santa Cruz, Santa Cruz, CA, USA
[140] Department of Physics, University of Washington, Seattle, WA, USA
[141] Department of Physics and Astronomy, University of Sheffield, Sheffield, UK
[142] Department of Physics, Shinshu University, Nagano, Japan
[143] Fachbereich Physik, Universität Siegen, Siegen, Germany
[144] Department of Physics, Simon Fraser University, Burnaby, BC, Canada
[145] SLAC National Accelerator Laboratory, Stanford, CA, USA
[146] [(a)]Faculty of Mathematics, Physics and Informatics, Comenius University, Bratislava, Slovak Republic; [(b)]Department of Subnuclear Physics, Institute of Experimental Physics of the Slovak Academy of Sciences, Kosice, Slovak Republic
[147] [(a)]Department of Physics, University of Cape Town, Cape Town, South Africa; [(b)]Department of Physics, University of Johannesburg, Johannesburg, South Africa; [(c)]School of Physics, University of the Witwatersrand, Johannesburg, South Africa

148 (a)Department of Physics, Stockholm University, Stockholm, Sweden; (b)The Oskar Klein Centre, Stockholm, Sweden
149 Physics Department, Royal Institute of Technology, Stockholm, Sweden
150 Departments of Physics and Astronomy and Chemistry, Stony Brook University, Stony Brook, NY, USA
151 Department of Physics and Astronomy, University of Sussex, Brighton, UK
152 School of Physics, University of Sydney, Sydney, SA, Australia
153 Institute of Physics, Academia Sinica, Taipei, Taiwan
154 Department of Physics, Technion: Israel Institute of Technology, Haifa, Israel
155 Raymond and Beverly Sackler School of Physics and Astronomy, Tel Aviv University, Tel Aviv, Israel
156 Department of Physics, Aristotle University of Thessaloniki, Thessaloníki, Greece
157 International Center for Elementary Particle Physics and Department of Physics, The University of Tokyo, Tokyo, Japan
158 Graduate School of Science and Technology, Tokyo Metropolitan University, Tokyo, Japan
159 Department of Physics, Tokyo Institute of Technology, Tokyo, Japan
160 Tomsk State University, Tomsk, Russia
161 Department of Physics, University of Toronto, Toronto, ON, Canada
162 (a)INFN-TIFPA, Trento, Italy; (b)University of Trento, Trento, Italy
163 (a)TRIUMF, Vancouver, BC, Canada; (b)Department of Physics and Astronomy, York University, Toronto, ON, Canada
164 Faculty of Pure and Applied Sciences, and Center for Integrated Research in Fundamental Science and Engineering, University of Tsukuba, Tsukuba, Japan
165 Department of Physics and Astronomy, Tufts University, Medford, MA, USA
166 Department of Physics and Astronomy, University of California Irvine, Irvine, CA, USA
167 (a)INFN Gruppo Collegato di Udine, Sezione di Trieste, Udine, Italy; (b)ICTP, Trieste, Italy; (c)Dipartimento di Chimica, Fisica e Ambiente, Università di Udine, Udine, Italy
168 Department of Physics and Astronomy, University of Uppsala, Uppsala, Sweden
169 Department of Physics, University of Illinois, Urbana, IL, USA
170 Instituto de Fisica Corpuscular (IFIC) and Departamento de Fisica Atomica, Molecular y Nuclear and Departamento de Ingeniería Electrónica and Instituto de Microelectrónica de Barcelona (IMB-CNM), University of Valencia and CSIC, Valencia, Spain
171 Department of Physics, University of British Columbia, Vancouver, BC, Canada
172 Department of Physics and Astronomy, University of Victoria, Victoria, BC, Canada
173 Department of Physics, University of Warwick, Coventry, UK
174 Waseda University, Tokyo, Japan
175 Department of Particle Physics, The Weizmann Institute of Science, Rehovot, Israel
176 Department of Physics, University of Wisconsin, Madison, WI, USA
177 Fakultät für Physik und Astronomie, Julius-Maximilians-Universität, Würzburg, Germany
178 Fakultät für Mathematik und Naturwissenschaften, Fachgruppe Physik, Bergische Universität Wuppertal, Wuppertal, Germany
179 Department of Physics, Yale University, New Haven, CT, USA
180 Yerevan Physics Institute, Yerevan, Armenia
181 Centre de Calcul de l'Institut National de Physique Nucléaire et de Physique des Particules (IN2P3), Villeurbanne, France

[a] Also at Department of Physics, King's College London, London, UK
[b] Also at Institute of Physics, Azerbaijan Academy of Sciences, Baku, Azerbaijan
[c] Also at Novosibirsk State University, Novosibirsk, Russia
[d] Also at TRIUMF, Vancouver BC, Canada
[e] Also at Department of Physics and Astronomy, University of Louisville, Louisville, KY, USA
[f] Also at Physics Department, An-Najah National University, Nablus, Palestine
[g] Also at Department of Physics, California State University, Fresno CA, USA
[h] Also at Department of Physics, University of Fribourg, Fribourg, Switzerland
[i] Also at Departament de Fisica de la Universitat Autonoma de Barcelona, Barcelona, Spain
[j] Also at Departamento de Fisica e Astronomia, Faculdade de Ciencias, Universidade do Porto, Portugal
[k] Also at Tomsk State University, Tomsk, Russia, Russia
[l] Also at The Collaborative Innovation Center of Quantum Matter (CICQM), Beijing, China
[m] Also at Universita di Napoli Parthenope, Napoli, Italy

[n] Also at Institute of Particle Physics (IPP), Victoria, BC, Canada
[o] Also at Horia Hulubei National Institute of Physics and Nuclear Engineering, Bucharest, Romania
[p] Also at Department of Physics, St. Petersburg State Polytechnical University, St. Petersburg, Russia
[q] Also at Department of Physics, The University of Michigan, Ann Arbor MI, USA
[r] Also at Centre for High Performance Computing, CSIR Campus, Rosebank, Cape Town, South Africa
[s] Also at Louisiana Tech University, Ruston LA, USA
[t] Also at Institucio Catalana de Recerca i Estudis Avancats, ICREA, Barcelona, Spain
[u] Also at Graduate School of Science, Osaka University, Osaka, Japan
[v] Also at Institute for Mathematics, Astrophysics and Particle Physics, Radboud University Nijmegen/Nikhef, Nijmegen, Netherlands
[w] Also at Department of Physics, The University of Texas at Austin, Austin TX, USA
[x] Also at Institute of Theoretical Physics, Ilia State University, Tbilisi, Georgia
[y] Also at CERN, Geneva, Switzerland
[z] Also at Georgian Technical University (GTU), Tbilisi, Georgia
[aa] Also at Ochadai Academic Production, Ochanomizu University, Tokyo, Japan
[ab] Also at Manhattan College, New York NY, USA
[ac] Also at Academia Sinica Grid Computing, Institute of Physics, Academia Sinica, Taipei, Taiwan
[ad] Also at School of Physics, Shandong University, Shandong, China
[ae] Also at Departamento de Fisica Teorica y del Cosmos and CAFPE, Universidad de Granada, Granada, Spain
[af] Also at Department of Physics, California State University, Sacramento CA, USA
[ag] Also at Moscow Institute of Physics and Technology State University, Dolgoprudny, Russia
[ah] Also at Departement de Physique Nucleaire et Corpusculaire, Université de Genève, Geneva, Switzerland
[ai] Also at Eotvos Lorand University, Budapest, Hungary
[aj] Also at Departments of Physics and Astronomy and Chemistry, Stony Brook University, Stony Brook NY, USA
[ak] Also at International School for Advanced Studies (SISSA), Trieste, Italy
[al] Also at Department of Physics and Astronomy, University of South Carolina, Columbia SC, USA
[am] Also at Institut de Física d'Altes Energies (IFAE), The Barcelona Institute of Science and Technology, Barcelona, Spain
[an] Also at School of Physics, Sun Yat-sen University, Guangzhou, China
[ao] Also at Institute for Nuclear Research and Nuclear Energy (INRNE) of the Bulgarian Academy of Sciences, Sofia, Bulgaria
[ap] Also at Faculty of Physics, M.V.Lomonosov Moscow State University, Moscow, Russia
[aq] Also at Institute of Physics, Academia Sinica, Taipei, Taiwan
[ar] Also at National Research Nuclear University MEPhI, Moscow, Russia
[as] Also at Department of Physics, Stanford University, Stanford CA, USA
[at] Also at Institute for Particle and Nuclear Physics, Wigner Research Centre for Physics, Budapest, Hungary
[au] Also at Giresun University, Faculty of Engineering, Turkey
[av] Also at Flensburg University of Applied Sciences, Flensburg, Germany
[aw] Also at CPPM, Aix-Marseille Université and CNRS/IN2P3, Marseille, France
[ax] Also at University of Malaya, Department of Physics, Kuala Lumpur, Malaysia
[ay] Also at LAL, Univ. Paris-Sud, CNRS/IN2P3, Université Paris-Saclay, Orsay, France
*Deceased